

DESIGN OF PID-BASED PNEUMATIC POSITION CONTROL IN LIFTING SYSTEM APPLICATION

LEE LING XUAN

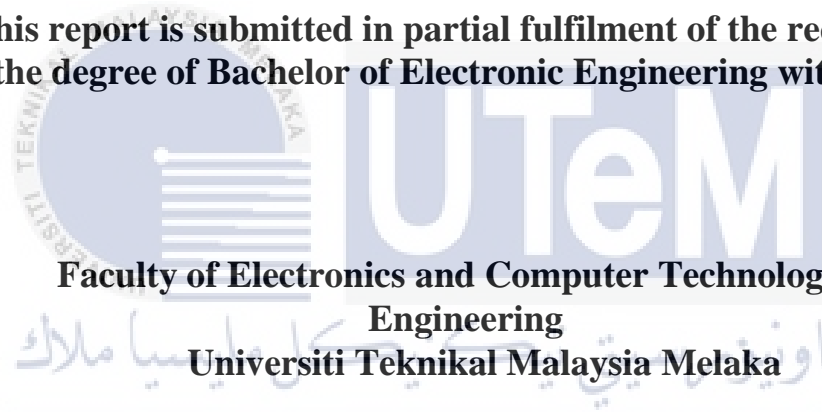


UNIVERSITI TEKNIKAL MALAYSIA MELAKA

**DESIGN OF PID-BASED PNEUMATIC POSITION
CONTROL IN LIFTING SYSTEM APPLICATION**

LEE LING XUAN

**This report is submitted in partial fulfilment of the requirements
for the degree of Bachelor of Electronic Engineering with Honours**



UNIVERSITI TEKNIKAL MALAYSIA MELAKA

2024

DECLARATION

I declare that this report entitled “Design of PID-Based Pneumatic Position Control in Lifting System Application” is the result of my own work except for quotes as cited in the references.



UNIVERSITI TEKNIKAL MALAYSIA MELAKA

Signature : 

Author : Lee Ling Xuan

Date : 19/06/2024

APPROVAL

I hereby declare that I have read this thesis and in my opinion, this thesis is sufficient in terms of scope and quality for the award of Bachelor of Electronic Engineering with Honours



Signature

اونيور سيتى فتم بى سوليمان
.....

Supervisor Name

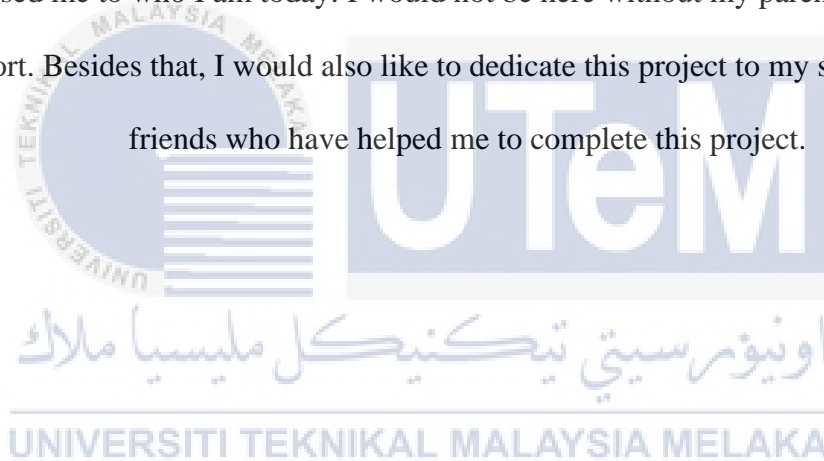
: Ts. Dr. Siti Fatimah Binti Sulaiman
.....

Date

: 20/06/2024
.....

DEDICATION

I would like to dedicate this project to my family especially my parents who has raised me to who I am today. I would not be here without my parents help and support. Besides that, I would also like to dedicate this project to my supervisor and friends who have helped me to complete this project.



ABSTRACT

The pneumatic lifting systems are crucial in industries like construction, manufacturing, and transportation for handling heavy loads. However, due to the non-linear behaviour of pneumatic systems, precise control is often difficult, leading to performance inconsistencies and safety risks. This research focuses on developing a Proportional-Integral-Derivative (PID) controller for an Intelligent Pneumatic Actuator (IPA) system. Using the System Identification technique, a 4th order Autoregressive with exogenous input (ARX) model was developed to accurately represent the dynamics of the system. The PID controller was designed and implemented in MATLAB/Simulink, achieving precise control characterized by fast response times and the absence of overshoot across various position distances of 50mm, 100mm and 150mm. Furthermore, the system maintained steady-state accuracy regardless of load variations from 1 kg to 5 kg. The results validate the effectiveness of the PID-based control strategy in enhancing the precision and accuracy of pneumatic lifting systems, contributing to more sustainable industrial operations.

ABSTRAK

Sistem pengangkatan pneumatik adalah penting dalam industri seperti pembinaan, pembuatan, dan pengangkutan untuk menangani beban berat. Walau bagaimanapun, disebabkan oleh kelakuan bukan linear sistem pneumatik, kawalan yang tepat sering kali sukar, yang menyebabkan ketidakkonsistenan prestasi dan risiko keselamatan. Penyelidikan ini memfokuskan kepada pembangunan pengawal terbitan-kamiran-berkadaran untuk sistem Penggerak Pneumatik Pintar (IPA). Menggunakan teknik Pengenalan Sistem, Model ARX tertib ke-empat telah dibangunkan untuk mewakili dinamik sistem dengan tepat. Pengawal PID direka dan dilaksanakan menggunakan MATLAB/Simulink, mencapai kawalan yang tepat dengan masa tindak balas yang cepat dan tanpa lebih dalam pelbagai jarak kedudukan 50mm, 100mm dan 150mm. Tambahan pula, sistem ini mengekalkan ketepatan keadaan mantap tanpa mengira variasi beban dari 1 kg hingga 5 kg. Hasilnya mengesahkan keberkesanan strategi kawalan berasaskan PID dalam meningkatkan ketepatan dan ketelitian sistem pengangkatan pneumatik, yang menyumbang kepada operasi industri yang lebih lestari.

ACKNOWLEDGEMENTS

I would like to express my deepest gratitude to my supervisor, Ts. Dr. Siti Fatimah Binti Sulaiman, whose guidance and support have been invaluable throughout this project. Her expertise, constructive feedback, and encouragement have greatly contributed to the successful completion of my work. I am particularly thankful for her patience and willingness to share her knowledge, which has significantly enhanced my understanding and skills.

I am also profoundly grateful to my parents for their unwavering support and encouragement. Their belief in my abilities and their constant motivation have been a source of strength for me. I cannot thank them enough for their love and support throughout my academic journey.

My heartfelt thanks go out to my friends, whose companionship and support have been instrumental during this challenging period. Lastly, I would like to extend my appreciation to Universiti Teknikal Malaysia Melaka (UTeM) for providing an excellent academic environment and resources that have been essential for the completion of my final year project.

TABLE OF CONTENTS

Declaration	
Approval	
Dedication	
Abstract	i
Abstrak	ii
Acknowledgements	iii
Table of Contents	iv
List of Figures	vii
List of Tables	ix
List of Symbols and Abbreviations	x
List of Appendices	xii
CHAPTER 1 INTRODUCTION	1
1.1 Overview	1
1.2 Problem Statement	3
1.3 Objectives	3
1.4 Scope of Work	4

1.5	Report Outline	5
CHAPTER 2 BACKGROUND STUDY		6
2.1	Overview of Pneumatic Actuator System	7
2.1.1	Intelligent Pneumatic Actuator (IPA) System	8
2.2	System Modeling of Pneumatic Actuator System	10
2.3	Control Strategies for Pneumatic Actuator System	16
2.4	Summary	24
CHAPTER 3 METHODOLOGY		26
3.1	Process Flowchart	26
3.2	Components of Intelligent Pneumatic Actuator (IPA) System	29
3.2.1	Programmable System on Chip (PSoC) Control Board	30
3.2.2	Pressure Sensor	31
3.2.3	Optical Encoder	31
3.2.4	Stripe Code	32
3.2.5	Valves	32
3.3	System Modeling Using System Identification Technique	33
3.3.1	Experimental Setup and Data Collection	33
3.3.2	Model Structure Selection	41
3.3.3	Model Estimation	45
3.3.4	Model Validation	46

3.4	Controller Design	48
3.5	Summary	51
CHAPTER 4 RESULTS AND DISCUSSION		52
4.1	System Modeling	53
4.1.1	Model Estimation	53
4.1.2	Model Validation	55
4.2	Position Control of IPA system	60
4.2.1	Simulation Experiment of IPA system	60
4.2.1.1	Simulation Experiment Performances and Analysis	63
4.2.2	Actual Experiment of IPA System	66
4.2.2.1	Actual Experiment Performances and Analysis	67
4.3	Position Control with Loading Effects	70
4.4	Environment and Sustainability	73
CHAPTER 5 CONCLUSION AND FUTURE WORKS		75
5.1	Conclusion	75
5.2	Future Works	76
5.2.1	Nonlinear Modeling	76
5.2.2	Advanced PID Control Techniques	76
REFERENCES		77
APPENDICES		83

LIST OF FIGURES

Figure 2.1	Components of IPA system [10]	9
Figure 3.1	Project flowchart	27
Figure 3.2	Components of IPA system	29
Figure 3.3	PSoC control board for IPA system	30
Figure 3.4	Pressure sensor for IPA system	31
Figure 3.5	Optical encoder for IPA system	31
Figure 3.6	Stripe code for IPA system	32
Figure 3.7	Valves for the IPA system	33
Figure 3.8	Experimental setup of IPA positioning system	34
Figure 3.9	Integration between the personal computer and the IPA system via the DAQ system	37
Figure 3.10	Connections of input and output device on SCB-68A	37
Figure 3.11	Input and output signals from the real-time experiment	39
Figure 3.12	Estimation and validation process of measured data	40
Figure 3.13	Block diagram of the ARX model structure	43
Figure 3.14	Block diagram of the ARMAX model structure	44
Figure 3.15	Orders of ARX model structure	44
Figure 3.16	Orders of ARMAX model structure	44
Figure 3.17	The model info after the process of estimating	46

Figure 3.18	Block diagram of PID controller	50
Figure 4.1	Plotting of best fit percentage for ARX model	55
Figure 4.2	Plotting of best fit percentage for ARMAX model	56
Figure 4.3	The pole-zero plot for 4 th order of ARX model	60
Figure 4.4	Control system of IPA system in simulation experiment	60
Figure 4.5	Controller parameters of the PID controller	62
Figure 4.6	Step response at position distance of 50 mm	63
Figure 4.7	Step response at position distance of 100 mm	64
Figure 4.8	Step response at position distance of 150 mm	64
Figure 4.9	Control system of IPA system in actual experiment	66
Figure 4.10	Step response at position distance of 50 mm	67
Figure 4.11	Step response at position distance of 100 mm	68
Figure 4.12	Step response at position distance of 150 mm	68
Figure 4.13	Pneumatic actuator with loads	70
Figure 4.14	Step response with 1kg load	71
Figure 4.15	Step response with 3kg load	71
Figure 4.16	Step response with 5kg load	72

LIST OF TABLES

Table 2.1	Comparison of specifications between pneumatic actuator system used in previous study and IPA system used in this study	10
Table 2.2	Summary of modeling techniques	14
Table 2.3	Summary of control strategies	22
Table 3.1	Cylinder stroke operation based on the condition of valves	36
Table 3.2	Specific terminal assignments for each input and output device on SCB-68A	38
Table 4.1	Transfer function of different orders ARX model	53
Table 4.2	Transfer function of different orders ARMAX model	54
Table 4.3	Summary of the best fit for ARX and ARMAX model	57
Table 4.4	The validation performance of ARX model structure for five different model orders	58
Table 4.5	The validation performance of ARMAX model structure for five different model orders	59
Table 4.6	Summary of the step response performances for position distance of 50 mm, 100 mm, and 150 mm in simulation experiment	64
Table 4.7	Summary of the step response performances for position distance of 50 mm, 100 mm, and 150 mm in actual experiment	69
Table 4.8	Summary of the step response performances for position control with loading effects of 1kg, 3kg and 5kg	72

LIST OF SYMBOLS AND ABBREVIATIONS

ARMAX	:	Auto-Regressive Moving Average with eXogenous input
ARX	:	Auto-Regressive with eXogenous input
BJ	:	Box-Jenkins
D	:	Derivative
DAQ	:	Data Acquisition
FPE	:	Final Prediction Error
FR	:	Filter-Regulator
I	:	Integral
I/O	:	Input/Output
IPA	:	Intelligent Pneumatic Actuator
MSE	:	Mean Square Error
OE	:	Output Error
P	:	Proportional
PI	:	Proportional-Integral
PID	:	Proportional-Integral-Derivative
PSoC	:	Programmable System on Chip
PWM	:	Pulse-Width Modulator
y	:	Actual measured data
\hat{y}	:	Predicted data from the model

\bar{y}	:	Mean of the actual measured data
σ^2	:	Variance of the residuals (errors)
OS	:	Overshoot
t_r	:	Rise Time
t_s	:	Settling Time
e_{ss}	:	Steady State Error



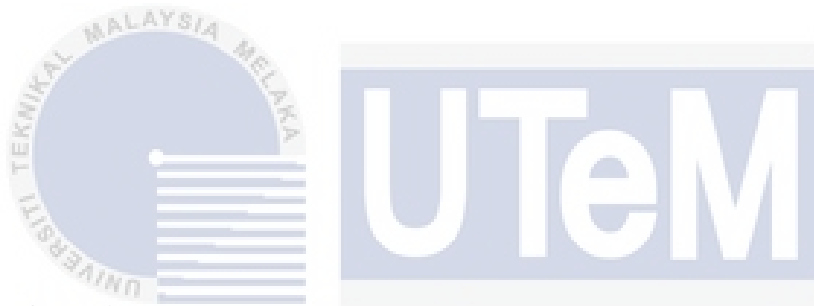
LIST OF APPENDICES

Appendix A	NI SCB-68A PINOUT	83
------------	-------------------	----



CHAPTER 1

INTRODUCTION



1.1 Overview

Lifting system is a mechanical setup used to raise and move heavy loads in various industrial settings like construction sites, manufacturing plants, and warehouses [1]. These systems are powered by different mechanisms such as pneumatic actuators (using compressed air), hydraulic systems (using fluid pressure), or electric motors. The primary function is to facilitate the safe and efficient handling of heavy objects, reducing manual labor and minimizing injury risks [2]. Effective lifting systems enhance productivity and safety, contributing to operational efficiency and longer equipment lifespans.

A pneumatic actuator system converts compressed air into mechanical motion, performing tasks such as moving or lifting objects. It operates by channeling

pressurized air into a cylinder, causing a piston to move and generate either linear or rotary motion. Known for their high-speed response, lightweight design, and simplicity, pneumatic actuators are widely used in industrial applications like robotics, manufacturing, and automation. They offer advantages such as cost-effectiveness, easy maintenance, and safety in high-temperature or explosive environments, making them a preferred choice for efficient and reliable motion control.

The Intelligent Pneumatic Actuator (IPA) system is chosen for this research due to its advanced capabilities in controlling pneumatic systems with enhanced precision and efficiency. The IPA system integrates sensors, controllers, and communication interfaces to monitor and adjust the actuator's performance in real-time. This intelligent approach allows for more accurate and responsive control of the actuator's movements, reducing the impact of the non-linear behavior typically seen in pneumatic systems. Additionally, the IPA system's ability to provide diagnostic and predictive maintenance features contributes to improved reliability and reduced downtime, making it an ideal choice for applications requiring high-performance and dependable motion control.

This project intends to develop a Proportional-Integral-Derivative (PID) controller specifically for pneumatic positioning systems in lifting applications to achieve precise control. Using the System Identification technique, a mathematical model that accurately represents the dynamics of the pneumatic lifting system will be developed. The PID controller, designed and implemented using MATLAB/Simulink, will ensure precise control over the lifting system. Analysis is then carried out for evaluating the transient response performance of the pneumatic positioning control system.

1.2 Problem Statement

Lifting systems are essential in various industries such as construction, manufacturing, and transportation, where they are used to handle heavy loads efficiently and safely. However, precise control of these systems remains challenging due to the non-linear behavior of pneumatic actuators, where the relationship between input and output is not always proportional. The increasing complexity of pneumatic actuators has led to the development of Intelligent Pneumatic Actuators (IPAs), which offer advanced features but also introduce new challenges. Modeling and controlling the IPA system is particularly difficult due to its complex nature, involving multiple unknown parameters and non-linear characteristics such as mass flow rate variations, dead zones, and compliance issues. These complexities, combined with constraints like friction, valve limitations, and the inherent weight of the system, can make the system unstable and complicate the control process.

The non-linearity and uncertainties within IPA systems can lead to inconsistent performance, posing significant safety risks and making robust performance difficult to achieve. To address these issues, this project aims to develop a Proportional-Integral-Derivative (PID) controller designed for pneumatic positioning systems to achieve precise control. By enhancing the precision and accuracy of these systems, the project seeks to improve operational safety, contributing to more sustainable industrial operations.

1.3 Objectives

- i. To develop a mathematical model that represents the dynamics of a pneumatic lifting system using System Identification technique.

- ii. To design and implement a Proportional-Integral-Derivative (PID) controller using MATLAB/Simulink to achieve precise control over the lifting system.
- iii. To evaluate and analyze the transient response performance of the pneumatic positioning control system.

1.4 Scope of Work

A new mathematical model for a pneumatic lifting system was developed using the System Identification technique, specifically considering linear model structures such as Auto-Regressive with eXogenous input (ARX) and Auto-Regressive Moving Average with eXogenous input (ARMAX) to accurately capture the characteristics of the system. The pressurized supply air was maintained at a constant 0.6 MPa throughout the experiments to ensure consistent conditions. A Proportional-Integral-Derivative (PID) controller was designed and implemented using MATLAB/Simulink to achieve precise control of the pneumatic system. The performance of the controller was rigorously tested for robustness by examining its response to load variations ranging from 1 kg to 5 kg.

The project was subject to certain limitations, particularly regarding the stroke length of the cylinder, which was restricted to 200 mm due to inherent constraints of the pneumatic system. This restriction ensured that the system operated within safe and effective parameters, allowing for a focused and manageable scope of study. By addressing these constraints and focusing on precise modeling and control, the project aimed to deliver a robust and reliable solution for pneumatic positioning control within the defined operational limits.

1.5 Report Outline

The report is organized into five chapters, each addressing different aspects of the project.

Chapter 1: Introduction covers the project's background, problem statement, objectives, scope of work, and report structure.

Chapter 2: Literature Review provides an overview of previous research on pneumatic actuator systems, focusing on the IPA system. It examines fundamental principles, industrial applications, advantages, limitations, modeling techniques, and control strategies used by previous researchers.

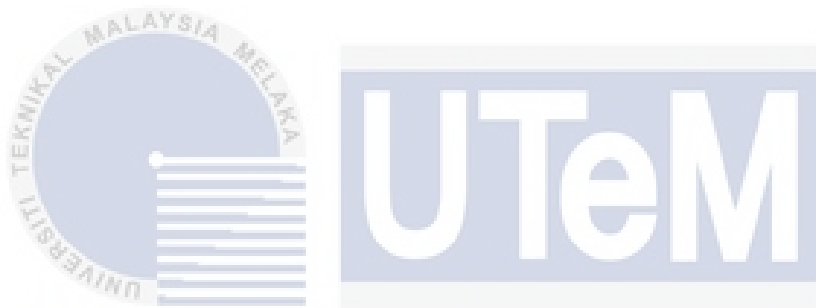
Chapter 3: Methodology outlines the methodology used in the project, starting with a study overview and flowchart. Details procedures for modeling the IPA positioning system using system identification and designing the PID controller.

Chapter 4: Results and Discussion presents system modeling results, including transfer functions for ARX and ARMAX models, with calculations of best fit, Mean Square Error (MSE), and Final Prediction Error (FPE). The chapter also compares simulation results with experimental data. The transient response is then analyzed and discussed in this chapter.

Chapter 5: Conclusion and Future Work summarizes findings and provides recommendations for future work.

CHAPTER 2

BACKGROUND STUDY



This chapter provides an overview of previous research on the pneumatic actuator system that is used in this study, specifically the IPA system. It begins by examining the fundamental principles and industrial applications of pneumatic actuators, highlighting their advantages and limitations. The chapter then discusses various techniques for modeling the pneumatic actuator system. Furthermore, the chapter also explores the control strategies that were employed by previous researchers.

2.1 Overview of Pneumatic Actuator System

Pneumatic actuator systems represent a fundamental mechanism in industrial automation, alongside hydraulic and electrical actuator systems [3]. Utilizing compressed air as their power source, pneumatic actuators consist of key components including pneumatic cylinders, valves, and control systems. These systems efficiently convert the energy from compressed air into linear or rotary motion, facilitating tasks such as valve control, component manipulation, and machinery automation across diverse industries.

Pneumatic actuator systems have several advantages that make them a preferred choice in many industrial applications. One of the key advantages is their simplicity. Pneumatic systems are relatively simple in design, comprising components such as cylinders, valves, and tubing, which are easy to install and maintain [4]. This simplicity reduces the complexity of setup, troubleshooting, and repair, ultimately lowering operational costs. Additionally, pneumatic actuators can achieve fast response times, making them suitable for applications requiring quick and precise motion [5]. With proper control, pneumatic systems can accelerate, decelerate, and reverse direction rapidly, enhancing productivity and efficiency in automated processes.

Another significant advantage of pneumatic actuator systems is their cost-effectiveness. Compared to hydraulic or electrical systems, pneumatic actuators often have lower initial costs [6]. The widespread availability of compressed air in industrial environments further contributes to their cost-effectiveness. Pneumatic systems are also inherently safer than some alternatives, particularly in hazardous environments. Since compressed air is non-toxic, non-flammable, and readily dissipates, the risk of

fire or environmental contamination is minimized. Furthermore, the robustness and ability of pneumatic actuators to withstand harsh operating conditions, including high temperatures[7] , moisture, and contamination, make them suitable for applications in industries such as manufacturing, mining, and automotive, where environmental challenges are common. Finally, pneumatic actuators can generate significant force relative to their size and weight, making them suitable for applications requiring compact and lightweight components[8]. This high power-to-weight ratio allows for efficient utilization of space and resources in industrial machinery and equipment.

Pneumatic actuator systems have several significant limitations. They are prone to leaks, leading to energy losses [9] and necessitating frequent maintenance to remain functional. While these systems can manage speed and position control, achieving high precision is more difficult compared to electric actuators because of the compressibility of air, which reduces control accuracy [10]. Additionally, the control of pneumatic actuators is complicated by nonlinearities and uncertainties such as valve response, friction, and the variable nature of air compressibility [11]. These factors make it hard to achieve consistent and reliable performance. Moreover, pneumatic systems are noisy due to the operation of compressors and air exhaust, making them less ideal for environments where low noise levels are important. These challenges collectively reduce the appeal of pneumatic systems in applications requiring high precision, reliability, and quiet operation.

2.1.1 Intelligent Pneumatic Actuator (IPA) System

The Intelligent Pneumatic Actuator (IPA) system is an advanced pneumatic actuation technology that integrates sensors, processors, and control mechanisms [12] to enhance the functionality and performance of pneumatic actuators. Unlike

traditional pneumatic actuators, which rely solely on compressed air for operation, IPAs incorporate intelligent features such as feedback control, monitoring, and adjustment capabilities[13]. These advanced functionalities enable IPAs to achieve higher levels of precision, efficiency, and reliability in various industrial applications. By continuously monitoring parameters such as position, force, and speed, IPAs can adapt to changing conditions in real-time, improving overall system performance [14] and responsiveness. This makes them suitable for a wide range of applications, including positioning, automation, and control systems where precise and dynamic actuation is required.

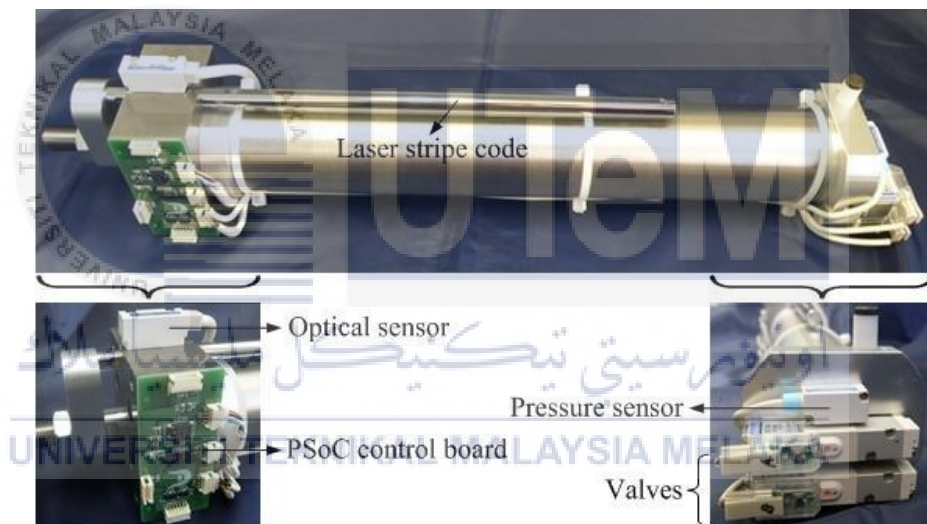


Figure 2.1 Components of IPA system [12]

Table 2.1 Comparison of specifications between pneumatic actuator system used in previous study and IPA system used in this study

Specifications	Pneumatic Actuator System used in previous study	IPA system used in this study
Stroke Length	50mm	200mm
Rod Diameter	20mm	16mm
Resolution	0.1mm	0.01mm
Picture		

Based on the details in Table 2.1, it is clear that the IPA system used in this study differs significantly from the pneumatic actuator system used in Pawlowski et al.'s earlier research [13]. The current IPA system has a longer stroke length of 200 mm. It also includes a position sensor with better accuracy and a new tape-type stripe code for greater durability. This IPA system offers much better positioning precision, being able to detect pitches as small as 0.01 mm. Essentially, this new IPA system addresses the issues of limited length and low accuracy that were present in the previous study.

2.2 System Modeling of Pneumatic Actuator System

System modeling involves both theoretical and experimental methods to accurately represent and predict the behavior of a system. The theoretical approach is

based on developing mathematical models that describe the system's dynamics through differential equations, state-space representations, or transfer functions. These models take into account the physical laws governing the system, such as Newton's laws for mechanical systems or Kirchhoff's laws for electrical circuits. Theoretical models are valuable for understanding fundamental system behaviors and for designing control strategies.

In contrast, the experimental approach involves collecting real-world data and using it to identify the system model. This process, known as system identification, involves applying specific inputs to the system and measuring the outputs. Various techniques, such as least squares estimation, are then used to derive mathematical models that fit the observed data. This approach is particularly useful for complex systems where theoretical modeling is challenging due to unknown parameters or unmodeled dynamics.

Sulaiman (2019) presented a mathematical model of the pneumatic actuator system used in this study. It was identified using an experimental method known as system identification. Data collection involved 1500 measurements of input and output data from a real-time experiment, with a sampling time of 0.01 seconds. The auto-regressive with exogenous input (ARX) parametric model was selected for this study as it met the criteria for system identification. A discrete state-space model based on the ARX structure was identified and used throughout the study, achieving a fit of approximately 91.09% to the actual plant model. The remaining 8.91% discrepancy may be attributed to factors such as dead zones, friction, and air leakage within the pneumatic system. The model is deemed stable as all poles and zeros are within the

unit circle. Therefore, the identified model is adequate for representing the pneumatic actuator system in this study [15].

Khong et al. (2020) discussed modeling a pneumatic actuator system with the ARX model structure. It suggests that due to the complexity of the system, an empirical approach is preferable over the complicated and exhaustive analytical method, even though nonlinearity is disregarded in the modeling assumption. In the third experiment, using input $u_2(t)$ yielded the highest best fit percentages of 93.04%, 93.10%, and 93.13%. Consequently, the ARX discrete polynomial model will use the estimated parameters from the configurations arx220, arx221, and arx222. However, for simplicity, the arx220 model will be chosen for simulation purposes [16].

Muftah (2021) presented different versions of the Intelligent Pneumatic Actuator (IPA) model, utilizing ARX, ARMAX, Box-Jenkins, Output-Error, and Hammerstein models. The IPA system model used in this analysis was created through an experimental method known as the system identification technique. The effectiveness of these models was assessed based on the most satisfactory output. The key finding of this research is that, among the models analyzed, the Hammerstein model structure achieved the highest percentage of best fit at 94.95%, outperforming ARX, ARMAX, OE, and BJ models. While ARX, ARMAX, OE, and BJ models also performed well, each achieving a best fit percentage exceeding 90%, the Hammerstein model proved to be better [17].

Awad (2021) introduced a method for controlling and identifying a servo pneumatic system within a mixed reality environment. A mathematical model is developed to analyze the system dynamics and nonlinear effects of the servo pneumatic system. The auto-regressive moving-average (ARMA) model-based

recursive least squares (RLS) algorithm is employed to determine the transfer function of the servo pneumatic system in real-time. Using the proposed ARMA model allows for effective and efficient identification of the system, ensuring high precision and minimal error, while also reducing the time required to adjust control unit parameters. The discrete transfer function of the servo pneumatic system is derived in real-time from the system's input and output data. Results from the identification process indicated that a fourth-order system model achieved the minimum square error with one-step prediction [18].

Etewa (2022) focused on developing a servo system model to enhance servo response through embedded circuit design. The identification of the black-box pneumatic servo system was conducted using MATLAB to aid in the embedded controller design. A MATLAB environment was created to perform system identification steps and derive transfer function models for the hardware using experimental data from a flight simulation model. The servo actuator's identified transfer function, initially in discrete form, was converted to a third-order continuous form. Various model structures, including ARX, ARMAX, Box-Jenkins (BJ), Output-Error (OE), and state space models were evaluated. The Box-Jenkins (BJ) model achieved the best fit with 92.29%, followed by ARMAX at 86.21%, ARX at 79.84%, and OE at 76.88% [19].

Kotkas et al. (2022) addressed the development of positioning control principles for a pneumatic artificial muscle (PAM) drive, focusing on both numerical and experimental investigations under various operational modes, such as lifting and lowering loads, handling sudden load separations, and manual operator force control. The study builds on a previously developed mathematical model, which includes static

and dynamic force models of the PAM. The dynamic model comprises differential equations that describe the muscle's movement, pressure changes in the bladder, and variations in force, volume, diameter, mesh angle, and bladder rigidity. The working principle of a PAM-actuated drive for an industrial manipulator is explored, with parameters adjusted from initial to pressurized states. Experimental validation confirms that the theoretical model accurately predicts both static and dynamic characteristics, making it suitable for designing PAM-based manipulators with specific performance requirements [20].

Mandali (2022) presented a robust cascade control system utilizing active disturbance rejection control (ADRC) for precise position control in pneumatic servo systems, characterized by nonlinearity, uncertainty, and disturbances. The control architecture includes an inner loop with a linear ADRC (LADRC) for valve position regulation and an outer loop with a nonlinear ADRC (NADRC) for controlling a nonlinear pneumatic actuator. The pneumatic system is modeled mathematically, incorporating piston-rod dynamics, pressure dynamics based on ideal gas law and mass conservation, and valve dynamics linked to mass flow rates and spool behavior. Simulation results confirm the proposed system's effectiveness and robustness, with stability of the control loops verified using a Lyapunov approach [21].

Table 2.2 Summary of modeling techniques

Author	Paper Title	Modeling Approach	Type of Models Used	Model with Highest Best Fit Percentage

Sulaiman (2019)	“A New Technique to Reduce Overshoot in Pneumatic Positioning System”	Experimental Approach	ARX	ARX, 91.09%
Khong et al. (2020)	“Linear ARX modelling of pneumatic actuator system”	Experimental Approach	ARX	ARX, 93.13%
Muftah (2021)	“ARX, ARMAX, Box-Jenkins, Output-Error, and Hammerstein Models for Modeling Intelligent Pneumatic Actuator (IPA) System”	Experimental Approach	ARX, ARMAX, OE, BJ & Hammerstein	Hammerstein 94.95%
Awad (2021)	“Identification and analysis of Servo-Pneumatic System using mixed reality environment”	Experimental Approach	ARMA	ARMA, fourth-order system model achieved the minimum square error

Etewa (2022)	“Design And Implementation of Embedded Servo Control System for a high maneuvering Ariel Vehicle”	Experimental Approach	ARX, ARMAX, OE, BJ & State Space	BJ, 92.29%
Kotkas et al. (2022)	“Design and Mathematical Modeling of a Pneumatic Artificial Muscle-Actuated System for Industrial Manipulators”	Theoretical Approach	Static and dynamic force models	-
Mandali (2022)	“Modeling and Cascade Control of a Pneumatic Positioning System”	Theoretical Approach	Piston-rod dynamics and pressure dynamics	-

2.3 Control Strategies for Pneumatic Actuator System

A controller for pneumatic actuator system is a crucial component in automation and control systems. It is a device or an algorithm that processes the input from sensors and generates the control output. This controller manipulates the pneumatic actuator system based on the feedback from the sensors, ensuring the system operates as desired. The controller’s main function is to maintain the stability

and performance of the system by adjusting the control variables based on the error between the desired and actual system output.

There are several types of controllers used in these systems, each with their unique characteristics and applications. PID (Proportional-Integral-Derivative) and PI (Proportional-Integral) controllers are commonly used due to their simplicity and effectiveness in various control situations. Fuzzy logic controllers use fuzzy sets and fuzzy logic rules instead of mathematical models, making them suitable for systems where precise mathematical models are difficult to obtain. Predictive controllers predict future outputs and adjust the control variables accordingly, while adaptive controllers adjust their parameters in real-time based on the system's behavior. Lastly, self-tuning controllers automatically tune their control parameters to optimize system performance, reducing the need for manual tuning. Each of these controllers plays a vital role in ensuring the efficient and reliable operation of pneumatic actuator systems.

Qi (2019) introduced a novel discrete-valued model-predictive control (DVMPC) algorithm, named DVMPC2, for the position control of pneumatic actuators using cost-effective on/off valves. DVMPC2 features a more adaptable cost function, enhanced prediction strategies, and various other improvements. The algorithm's performance was experimentally compared to the state-of-the-art sliding-mode control (SMC) algorithm and the previous DVMPC version. Evaluation metrics included the integral of time-weighted absolute error (ITAE), root mean square error (RMSE), overshoot (OS), steady-state error (SSE), and valve switches per second (SPS). Robustness was tested by varying the total mass of moving components while maintaining constant controller parameters. Experimental results demonstrated that

DVMPC2 significantly outperforms both its predecessor and the SMC algorithm, reducing ITAE by 80%, RMSE by 52%, OS by 43%, and SPS by 20%, with an SSE of 0.578 mm [22].

Youssry (2020) proposed an improved PWM positioning control algorithm for a double-acting pneumatic cylinder, achieving satisfactory accuracy and enabling the use of cost-effective commercial components instead of expensive ones. The enhanced algorithm incorporates a dead-zone compensator and utilizes optimal pneumatic parameter values obtained from a prior parametric study, effectively mitigating the system's nonlinear dynamics. This modified approach significantly improves system performance, reducing the steady-state error from ± 2.5 mm with the traditional PWM control algorithm to ± 0.28 mm [23].

Azahar et al. (2020) proposed a cascade control technique called Fuzzy Self-Adaptive PID (CFSAPID) control. This approach employs a Fuzzy Logic Controller (FLC) to dynamically tune the PID controller. The effectiveness of the proposed CFSAPID is evaluated through simulations on a single-piston double-acting valve pneumatic system model and compared with a single FSAPID controller. Key performance metrics analyzed include piston rise time, piston settling time, piston velocity, pressure in the piston chambers, and frictional force. Simulation results demonstrate that the CFSAPID significantly outperforms the FSAPID, achieving a steady-state error of 0.0109 mm compared to 0.3357 mm for the FSAPID [24].

El-sayed and Hammam (2020) presented both simulation and experimental investigations into the position control of pneumatic cylinders. Instead of using a proportional control valve, a high-speed on-off solenoid air valve is employed. A sliding mode control with error modification (SMCE) is proposed to operate the air

valves using a pulse width modulation (PWM) technique. The performance of the closed-loop position control using SMCE is compared with that of a traditional PID controller. The simulation model is utilized to optimize the parameters for both SMC and PID controllers before commencing experimental tests. Experimental results for square and sinusoidal position references indicate that SMCE outperforms the PID controller, exhibiting lower steady-state errors, faster settling times, and reduced overshoot. Specifically, the steady-state error achieved by SMCE is 0.22 mm, compared to 0.69 mm for the PID controller [25].

Lateef et al. (2020) has developed a cost-effective electro-pneumatic module suitable for use in industrial automation equipment, robotic systems, and mechatronic applications. A Pulse Width Modulation (PWM) technique is employed to accurately control the piston position, enabling the system to follow desired trajectories precisely across various applications. This approach presents a low-cost alternative to using proportional valves in electro-pneumatic systems. A Fuzzy Logic algorithm combined with PD control is implemented in the Matlab/Simulink environment to adjust control values. The simulation results and model responses were compared with previous practical results using a similar model and controller but equipped with a proportional valve. The comparison showed that the simulation results closely matched the practical outcomes, with steady-state errors of 0.48 mm in practical tests and 0.5 mm in simulations[26].

Kamaludin (2021) implemented a Proportional-Integrator (PI) controller with a "zero-compensator" using the zero-placement method to simplify the control process. This controller is more straightforward, functional, and practical than other complex controllers. Simulations show that the PI controller with zero-compensator

significantly improves the servo pneumatic system's response. Specifically, it enhances rise time (TR) by 66.22%, reduces percent overshoot (%OS) by 96.49%, and decreases settling time (TS) by 89.12%. Both the PI controller and the PI with zero-compensator achieve a steady-state error of 0. Comprehensive transient response parameters were validated to support the analysis[27].

Sulaiman (2021) introduced a novel approach to improve pneumatic positioning systems while considering system constraints. First, a mathematical model of the pneumatic system was established using a system identification approach. Then, a model predictive controller (MPC) was developed as the primary controller, incorporating system constraints. To further enhance performance, a nonlinear gain function was integrated into the MPC algorithm. The performance of this enhanced MPC was compared with other control methods, including constrained MPC (CMPC), proportional-integral (PI), and predictive functional control with observer (PFC-O). Real-time experimental results for 100 mm positioning control demonstrated that the MPC algorithm with nonlinear gain improved speed response by 21.03% and 2.69% compared to CMPC and PFC-O, respectively, and completely eliminated overshoot compared to CMPC and PI controllers. The CMPC achieved a steady-state error of 0. These results indicate that the proposed approach provides a fast and accurate pneumatic positioning control system[28].

Muftah et al. (2022) focused on reducing the overshoot in the response time of a double-acting pneumatic actuator, specifically within the IPA positioning system. The pneumatic system was modeled using an autoregressive with exogenous input (ARX) model structure. The control strategy implemented was a fuzzy fractional order proportional integral derivative (fuzzy FOPID) controller optimized by the particle

swarm optimization (PSO) algorithm, which was used to determine the optimal controller parameters. A comparative study was conducted to demonstrate the benefits of the PSO fuzzy FOPID controller over the PSO fuzzy PID controller. The tuning algorithm for the controller was validated and tested on a pneumatic actuator system in both simulation and real-world environments. Regarding time-domain performance metrics such as rise time (t_r), settling time (t_s), and overshoot ($OS\%$), the PSO fuzzy FOPID controller showed superior dynamic performance, achieving a steady-state error of 0 mm compared to the PSO fuzzy PID controller [29].

MinZhu et al. (2022) proposed a new valve position control method utilizing a fractional-order PID controller. This method begins with an analysis of the working principle of a pneumatic control valve and the establishment of its mathematical model. To enhance the model's accuracy, an improved biogeography-based optimization (IBBO) algorithm is introduced for tuning the parameters of the fractional-order PID controller, addressing the broad range and high complexity of this controller type. Simulation and experimental results demonstrate that the fractional-order PID controller outperforms the traditional integer-order PID controller in terms of response speed and control accuracy, making it more suitable for pneumatic control valve position control. Specifically, the IBBO-FOPID control algorithm achieved an overshoot of just 0.6760% and a steady-state error of 0.0008 in simulations[30].

Muftah (2023) focused on enhancing the performance of a pneumatic positioning system by developing a control system based on Fuzzy Fractional Order Proportional Integral Derivative (Fuzzy FOPID) controllers. The mathematical model of the pneumatic system was derived using a system identification approach, and the

Fuzzy FOPID controller was optimized with a Particle Swarm Optimization (PSO) algorithm to ensure a balance between performance and robustness. The system's performance was then compared to that of a Fuzzy PID controller through real-time experiments, which revealed that the Fuzzy FOPID controller provided superior speed, stability, and precision. The proposed control system was tested on a pneumatically actuated ball and beam (PABB) system, employing a Fuzzy FOPID controller for both the inner and outer loops. All control strategies achieved zero steady-state error across all distances, confirming their effectiveness in providing precise positioning control for the IPA system [31].

Table 2.3 Summary of control strategies

Author	Paper Title	Control Method	Steady-State Error (mm)
Qi (2019)	“Position control of pneumatic actuators using three-mode discrete-valued model predictive control”	Discrete-Valued Model-Predictive Control (DVMPC)	0.578
Youssry (2020)	“Position control of a pneumatic cylinder actuator using modified PWM algorithm”	Modified PWM Algorithm	0.28
Azahar et al. (2020)	“Position Control of Pneumatic Actuator Using Cascade Fuzzy Self-adaptive PID”	Cascade Fuzzy Self-Adaptive PID (CFSAPID)	0.0109

El-sayed and Hamman (2020)	“Simulation Study and Experimental Position Control of Pneumatic Cylinder Using Sliding Mode Control with on/off Control Valves”	Sliding Mode Control with Error Modification (SMCE)	0.22
Lateef et al. (2020)	“Modelling and Controlling of position for electro-pneumatic system using Pulse-Width-Modulation (PWM) techniques and Fuzzy Logic controller”	Fuzzy Logic Controller	0.48
Kamaludin (2021)	“Improvement of a Proportional-Integral (PI) Controller for a Servo Pneumatic Actuator by Adapting Zero-Compensator Placement Method”	Proportional-Integrator (PI) Controller	0
Sulaiman (2021)	“Enhancement in pneumatic positioning system using nonlinear gain constrained model predictive controller: Experimental validation”	Constrained Model Predictive Controller (CMPC)	0
Muftah et al. (2022)	“Modeling and Fuzzy FOPID Controller Tuned by PSO for	Fuzzy Fractional Order Proportional	0

	Pneumatic Positioning System”	Integral Derivative (Fuzzy FOPID)	
MinZhu et al. (2022)	“Design of FOPID Controller for Pneumatic Control Valve Based on Improved BBO Algorithm,”	Fractional Order PID Controller (FOPID)	0.0008
Muftah (2023)	“Fuzzy Fractional Order PID Tuned via PSO for a Pneumatic Actuator with Ball Beam (PABB) System”	Fuzzy Fractional Order Proportional Integral Derivative (Fuzzy FOPID) Controller	0

2.4 Summary

This chapter reviews existing research on the pneumatic actuator systems and Intelligent Pneumatic Actuator (IPA) systems. The IPA system was selected over pneumatic actuator systems due to its enhanced precision, reliability, and suitability for complex tasks such as lifting and positioning control. Traditional pneumatic actuators often struggle with issues like nonlinearity and sensitivity to external disturbances, whereas IPA systems are designed to mitigate these challenges, offering superior performance and control accuracy in industrial applications.

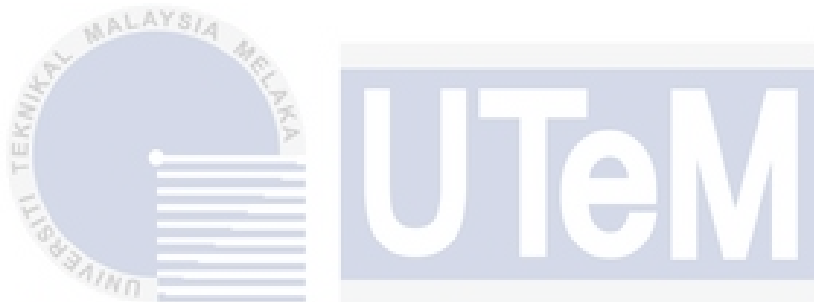
The study focuses on an experimental approach rather than a theoretical one. This choice is based on the need to develop a model that accurately reflects the real-world behavior and dynamics of the system. By using experimental methods, specifically system identification, the model is derived from actual data collected from

the IPA system during operation. This approach ensures that the control strategies are based on realistic and practical system behavior, leading to more effective and reliable control solutions compared to theoretical models, which may not fully capture the complexities of the physical system.

The model of the IPA system was obtained using the System Identification (SI) method, with the Auto-Regressive with Exogenous Input (ARX) model being employed. The ARX model was chosen due to its simplicity and effectiveness in capturing the linear dynamics of the system by incorporating both past inputs and outputs. This makes it particularly suitable for identifying the input-output relationships in the IPA system. The control strategy implemented in this study is based on the PID controller, which is well-known for its robustness, simplicity, and effectiveness. The PID controller's ability to adjust proportional, integral, and derivative gains allows for fine-tuning of the system's response, minimizing steady-state error, and optimizing overall performance in positioning control applications.

CHAPTER 3

METHODOLOGY



This chapter outlines the methodology used in completing this project. The chosen methods are based on background studies and reviews of prior research. The chapter starts with a brief overview of the study, illustrated with a flowchart. It then details the procedures for modeling the Intelligent Pneumatic Actuator (IPA) positioning system using a system identification approach. Finally, the chapter explains the methodology for designing the PID controller to control the IPA positioning system.

3.1 Process Flowchart

This study is comprised of four main stages which are literature review, system modeling, controller design and simulation testing, and performance analysis. Figure 3.1 shows the process flow of the study.

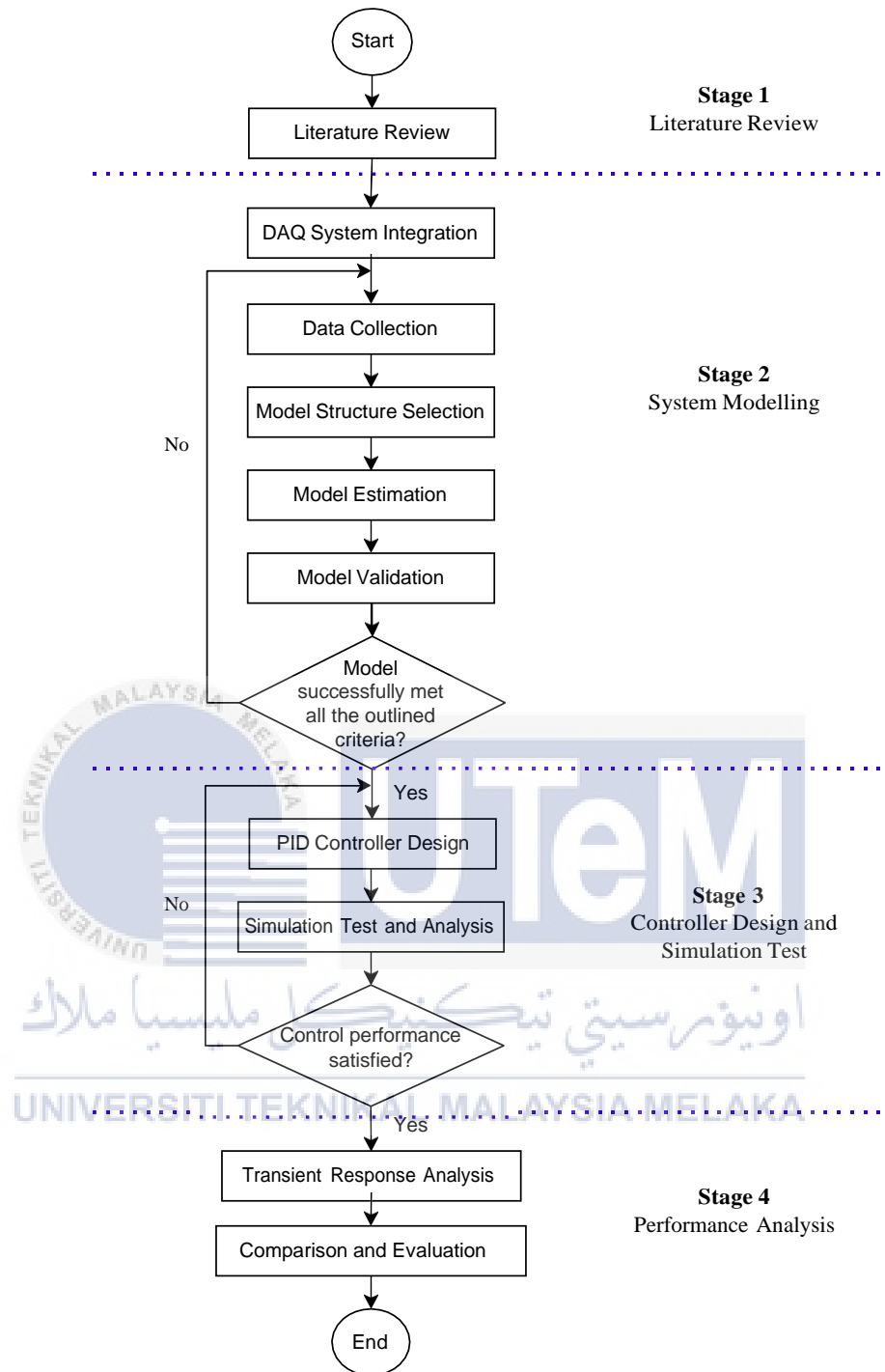


Figure 3.1 Project flowchart

In the initial stage, a comprehensive literature review is conducted to gather relevant information and insights on the Intelligent Pneumatic Actuator (IPA) positioning system. This involves examining previous research studies, technical

papers, and related works to identify the main challenges and issues associated with controlling the IPA system. The objective is to understand the existing knowledge base and pinpoint the gaps that need to be addressed in this study. By doing so, the review helps in formulating the research questions and hypotheses, as well as establishing a solid foundation for the empirical approach that follows. The findings from the literature review guide the selection of methodologies and inform the overall direction of the project.

In stage 2, system modeling begins with the integration of a Data Acquisition (DAQ) system, which is essential for collecting precise input and output data from the IPA system. This data collection process involves conducting experimental work where the measured inputs (such as control signals) and outputs (such as the position of the actuator) are recorded. These experimental measurements are crucial for developing an accurate mathematical representation of the IPA system. The Auto-Regressive with eXogenous input (ARX) model structure is selected for this purpose due to its ability to effectively capture the dynamics of the system. The collected data is then used to estimate the parameters of the ARX model, resulting in a mathematical model that approximates the real behavior of the IPA system. Lastly, this model undergoes validation to ensure its accuracy and reliability in predicting the system's behavior, thus confirming its suitability for controller design.

In stage 3, a Proportional-Integral-Derivative (PID) controller is designed to improve the transient response of the IPA system, aiming for precise and accurate position control. The design process involves selecting appropriate PID parameters that will enable the controller to achieve desired performance characteristics, such as minimizing overshoot and steady-state error. MATLAB/Simulink is employed to

simulate the behavior of the PID-controlled IPA system, allowing for a detailed analysis of the controller's performance in a virtual environment. This simulation stage is crucial as it enables the identification and rectification of potential issues before physical implementation. Through iterative testing and refinement, the PID controller is fine-tuned to optimize its performance.

The final stage focuses on the performance analysis of the proposed control strategy. This involves conducting experimental tests where different load variations, ranging from 1 kg to 5 kg, are applied to the IPA system to assess the controller's accuracy and robustness in maintaining its position. The transient response of the system is analyzed in detail to determine how well the PID controller performs in real-world conditions. Once the controller satisfies these requirements, the study concludes with a comprehensive evaluation of the control strategy's effectiveness, highlighting its potential applications and benefits in practical scenarios.

3.2 Components of Intelligent Pneumatic Actuator (IPA) System

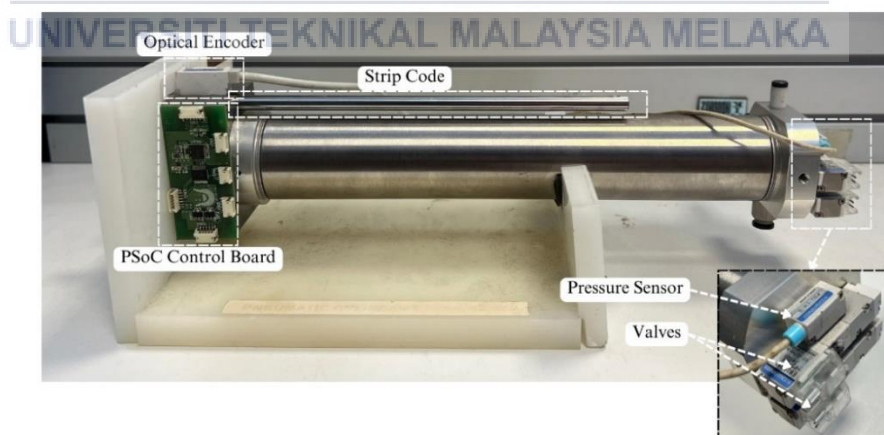


Figure 3.2 Components of IPA system

The Intelligent Pneumatic Actuator (IPA) system in this study utilizes a double-acting cylinder with the following specifications: it operates using air as the

medium, within a pressure range of 0.1 to 0.7 MPa. The cylinder has a bore size of 40 mm, a stroke length of 200 mm, and a rod diameter of 16 mm. At an operating pressure of 0.6 MPa, the cylinder can exert a maximum force of 120 N. This double-acting cylinder, specifically a KOGANEI-HA twin port cylinder, is equipped with two air inlets and one exhaust outlet, making it suitable for precise and controlled movements in the IPA system.

3.2.1 Programmable System on Chip (PSoC) Control Board

The Programmable System on Chip (PSoC) control board is a vital component of the IPA system, responsible for the control and communication functions of the actuator. It includes connectors for communication, power supply, programming, and interfacing with IPA sensors and valves, as depicted in Figure 3.3. The board features several integrated components, such as the PSoC chip, voltage regulator, Darlington pair, and LEDs. It processes input signals from the optical encoder and pressure sensor, and outputs PWM signals to control the valves and LEDs.

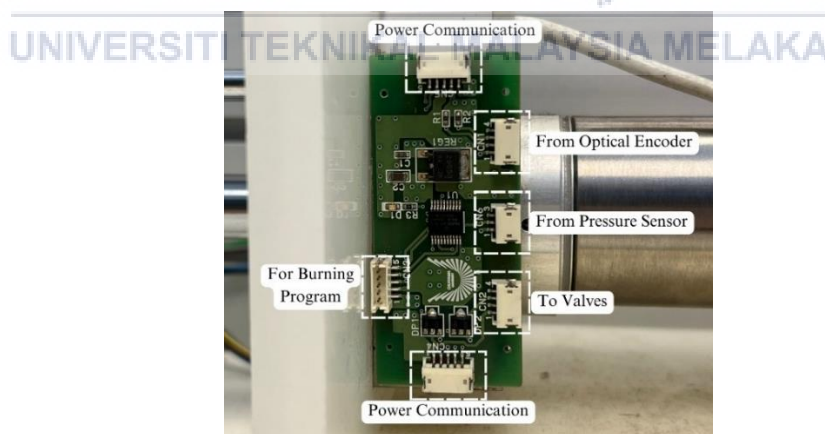


Figure 3.3 PSoC control board for IPA system

3.2.2 Pressure Sensor

The pressure sensor employed in this study is the KOGANEI PSU-EM-S model. It measures the pressure within the cylinder chamber and sends the data to the PSoC control board for processing and control actions. Positioned at the end of the cylinder, along with the valves, the sensor plays a crucial role in monitoring and maintaining the system's pressure levels.



Figure 3.4 Pressure sensor for IPA system

3.2.3 Optical Encoder

The optical encoder used in this study is the KOGANEI ZMA1R model, mounted at the top of the actuator. It detects the position of the cylinder stroke by reading the laser stripes on a guide rod attached to the actuator. The encoder transmits these position readings to the PSoC control board for further processing. The sensor can accurately detect strokes with a resolution as small as 0.01 mm. To ensure precise readings, a specific gap is maintained between the encoder and the laser stripes. This setup allows for highly accurate position detection of the IPA cylinder stroke.

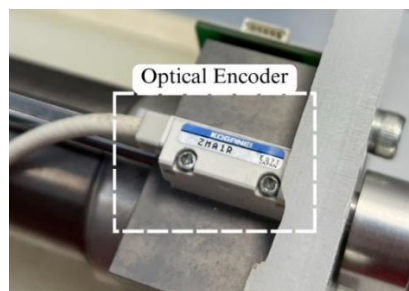


Figure 3.5 Optical encoder for IPA system

3.2.4 Stripe Code

The stripe code used in this study is a tape type with a 0.01 mm pitch, as illustrated in Figure 3.6. The tape is placed on the guide rod and contains stripes created by irradiating a Yttrium Aluminum Garnet (YAG) laser beam, which oxidizes the tape surface. The optical encoder reads these stripe codes to determine the position of the IPA cylinder stroke with high precision. The small pitch of the stripes enhances the positioning accuracy of the system, enabling the encoder to detect very fine movements of the actuator.

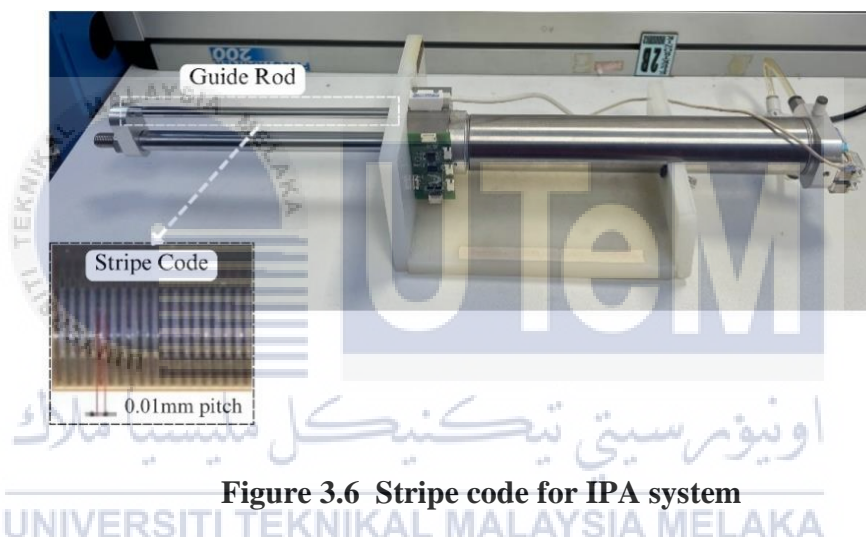


Figure 3.6 Stripe code for IPA system

3.2.5 Valves

The IPA system uses two KOGANEI EB10SA1-PS-6W valves. These valves control the air inlet and outlet of the cylinder and are positioned at the end of the cylinder, as shown in Figure 3.7. The valves are driven by Pulse-Width Modulated (PWM) signals, which control the extension and retraction of the cylinder stroke by manipulating the duty cycle. The actuator operates at a frequency of 20 Hz, which is factored into the duty cycle calculation for precise control of the valve movements.

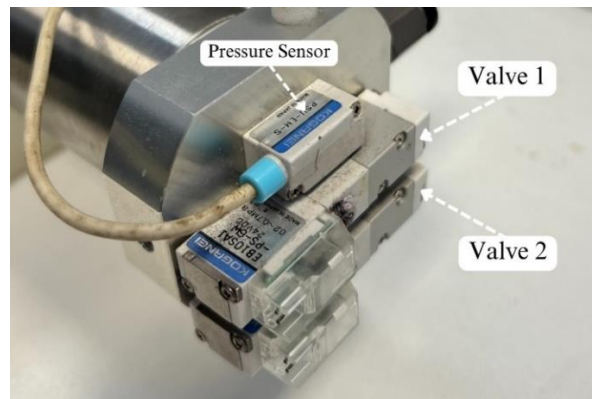


Figure 3.7 Valves for the IPA system

3.3 System Modeling Using System Identification Technique

System modeling using the system identification technique is a method for developing mathematical models of dynamic systems based on measured data. In the context of the Intelligent Pneumatic Actuator (IPA) positioning system, this approach involves several key steps:

1. Experimental Setup and Data Collection
2. Model Structure Selection
3. Model Estimation
4. Model Validation

3.3.1 Experimental Setup and Data Collection

Figure 3.8 shows the experimental setup of the Intelligent Pneumatic Actuator (IPA) positioning system involves several key components working together to ensure precise control and accurate data collection.

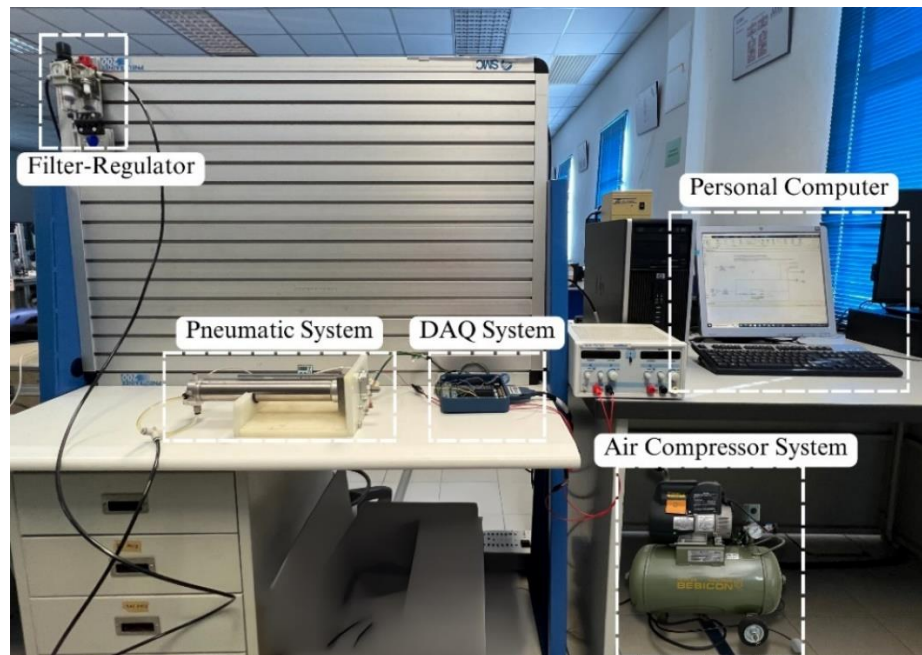


Figure 3.8 Experimental setup of IPA positioning system

At the core of the setup is a personal computer, which serves as the primary interface for system control and data analysis. The computer runs software such as MATLAB/Simulink, which is used to simulate the control algorithms and process the data collected from the IPA system.

The air compressor system supplies the necessary pneumatic power to the IPA system. In this study, an industrial-grade air compressor is used, providing a pressurized air supply at 0.6 MPa. To ensure the air supply is clean and free of contaminants, a Filter-Regulator (FR) unit is employed. The FR unit filters out impurities and regulates the air pressure to maintain consistent and optimal operating conditions for the IPA system.

The primary component of the experimental setup is the IPA system itself. This system includes the double-acting pneumatic cylinder, optical encoder, stripe code, pressure sensor, and valves. The double-acting cylinder operates with two air inlets

and one exhaust outlet, enabling controlled movement of the actuator rod. The optical encoder, mounted at the top of the actuator, reads the position of the cylinder stroke with high precision by detecting laser stripes on a guide rod. The pressure sensor monitors the air pressure within the cylinder chamber, providing crucial data for system control.

The extension and retraction of the cylinder stroke in the Intelligent Pneumatic Actuator (IPA) system are controlled by two valves, each regulated by a Pulse-Width Modulated (PWM) signal. The PWM module provides an 8-bit precision, which translates to signal values ranging from +255 to -255.

When extending the cylinder stroke, the control system sends a positive PWM signal, close to +255, to Valve 1. This signal fully opens Valve 1, allowing pressurized air from the air compressor to flow into the front chamber of the double-acting cylinder. At the same time, Valve 2, responsible for exhausting air from the rear chamber, remains closed. The influx of pressurized air into the front chamber creates a force that pushes the piston rod outward, resulting in the extension of the cylinder stroke.

Conversely, to retract the cylinder stroke, the control system sends a negative PWM signal, close to -255, to Valve 2. This signal fully opens Valve 2, allowing the pressurized air in the rear chamber to be exhausted out of the cylinder. Simultaneously, Valve 1 remains closed, preventing additional air from entering the front chamber. As the rear chamber depressurizes, the differential pressure between the two chambers causes the piston rod to move back into the cylinder, thus retracting the cylinder stroke.

The precision of the 8-bit PWM module, which allows for 256 discrete levels of control, enables fine adjustment of the valves' openings. This level of control is crucial for achieving smooth and precise movements of the actuator. By varying the duty cycle of the PWM signals, the system can modulate the flow rates through the valves, thereby controlling the speed and position of the cylinder stroke accurately.

Table 3.1 Cylinder stroke operation based on the condition of valves

Cylinder Stroke Operation	Valve Condition	
	Valve 1	Valve 2
No Operation	OFF	OFF
Extension	ON	OFF
Retraction	OFF	ON
No Operation	ON	ON

In the experimental setup for the Intelligent Pneumatic Actuator (IPA) positioning system, the integration between the personal computer and the IPA system is achieved using a Data Acquisition (DAQ) system. This setup ensures precise control and accurate data collection, facilitated by MATLAB and Simulink software running on the personal computer.

The DAQ system used in this study includes the NI-DAQ system (model PCI-6221), the SHC68-68-EPM cable, and the SCB-68A connector block as shown in Figure 3.9. The PCI-6221 DAQ card is installed in the personal computer, providing the necessary interface for converting digital signals to analog signals and vice versa. The SHC68-68-EPM cable connects the DAQ card to the SCB-68A connector block,

which serves as the terminal for connecting various sensors and actuators of the IPA system.

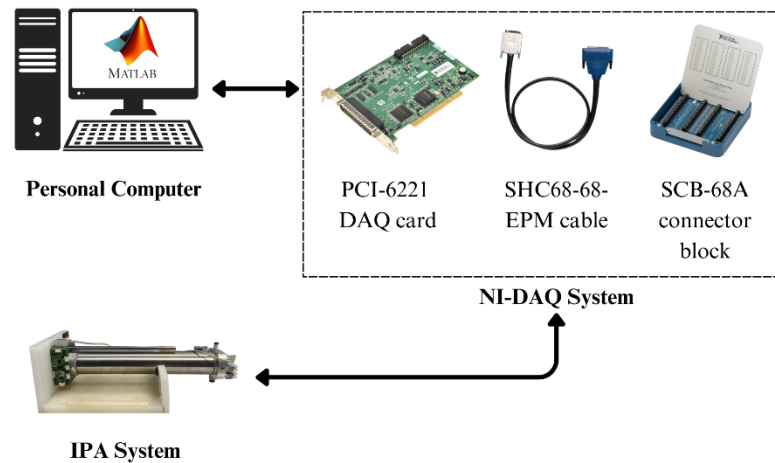


Figure 3.9 Integration between the personal computer and the IPA system via the DAQ system

The SCB-68A connector block from National Instruments is a shielded I/O device designed for secure and reliable connections between measurement devices and DAQ hardware. Featuring 68 pins and screw-terminal connections, it ensures noise-free signal transmission and easy wiring of sensors and actuators. In the IPA positioning system, the SCB-68A facilitates connections for valves, pressure sensors, and optical sensors as shown in Figure 3.10.

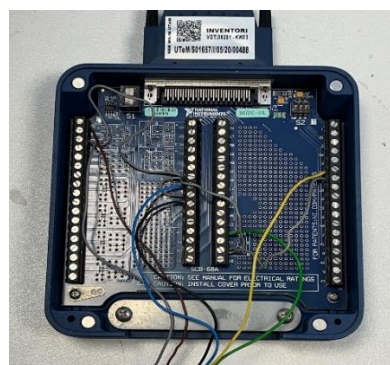


Figure 3.10 Connections of input and output device on SCB-68A

Table 3.2 Specific terminal assignments for each input and output device on SCB-68A

Input and Output Device	Signal Terminal Number	Ground Terminal Number
Optical Sensor CH-A	37 (PFI 8/P2.0)	4
Optical Sensor CH-B	45 (PFI 10/P2.2)	44
Pressure Sensor	68 (AI 0)	67
Valve 1	21 (AO 1)	55
Valve 2	22 (AO 0)	56

Table 3.2 shows the configuration of the SCB-68A connector block includes specific terminal assignments for each input and output device, ensuring accurate signal processing and control.

The real-time data collected from the sensors is processed in MATLAB /Simulink to monitor the system's performance and make necessary adjustments to the control signals. This feedback loop ensures that the IPA system operates smoothly and accurately, achieving the desired positioning control.

In this study, an open-loop experimental test was conducted three times to ensure reliable data extraction and consistent input-output performance. The experiments spanned 15 seconds with a sampling time (T_s) of 10 milliseconds. The choice of a 10ms sampling time was justified for several reasons. Firstly, it allows for the collection of more data samples for the model identification process. Secondly, it aligns with the hardware specifications and limitations of the DAQ and IPA systems.

Lastly, best practices suggest that the sampling time should be 10 times faster than the processing time constant. A longer sampling time could lead to significant modeling errors due to lost or missed key information. Figure 3.11 illustrates the measured input and output data from the real-time experiment.

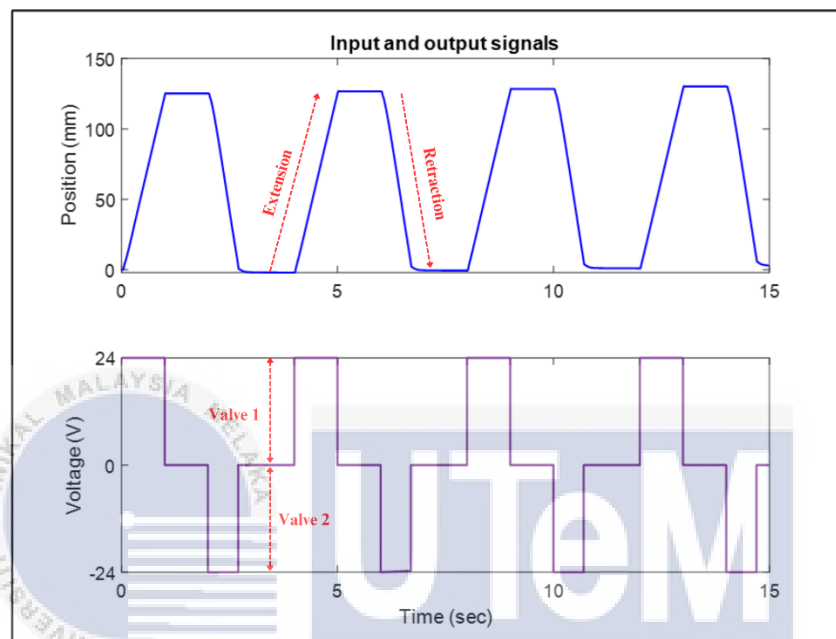


Figure 3.11 Input and output signals from the real-time experiment

Figure 3.11 illustrates the relationship between the input signals to the valves and the corresponding cylinder stroke position over a 15-second period. The upper plot shows the position of the cylinder in millimeters, while the lower plot depicts the voltage signals sent to the two valves.

In the lower plot, Valve 1 and Valve 2 are operated by PWM signals at 24 V. When a positive voltage is applied (indicated as the positive amplitude), Valve 1 is activated, controlling the air inlet to extend the cylinder. Conversely, when a negative voltage is applied, Valve 2 is activated, controlling the air outlet to retract the cylinder. The alternating pattern of positive and negative voltages corresponds to the cyclical

extension and retraction of the cylinder, as depicted in the upper plot. The data acquisition system (ADC) captures these signals, converting them to a format suitable for the PWM module, which then precisely controls the valves based on the input signals. The graph clearly shows the periodic nature of the cylinder's motion, driven by the alternating control of the two valves.

In this study, data collection involved 1500 measurements of input and output signals. The collected data is divided into two sets using MATLAB System Identification Tool as shown in Figure 3.12. The model estimation and validation were conducted using the collected data.

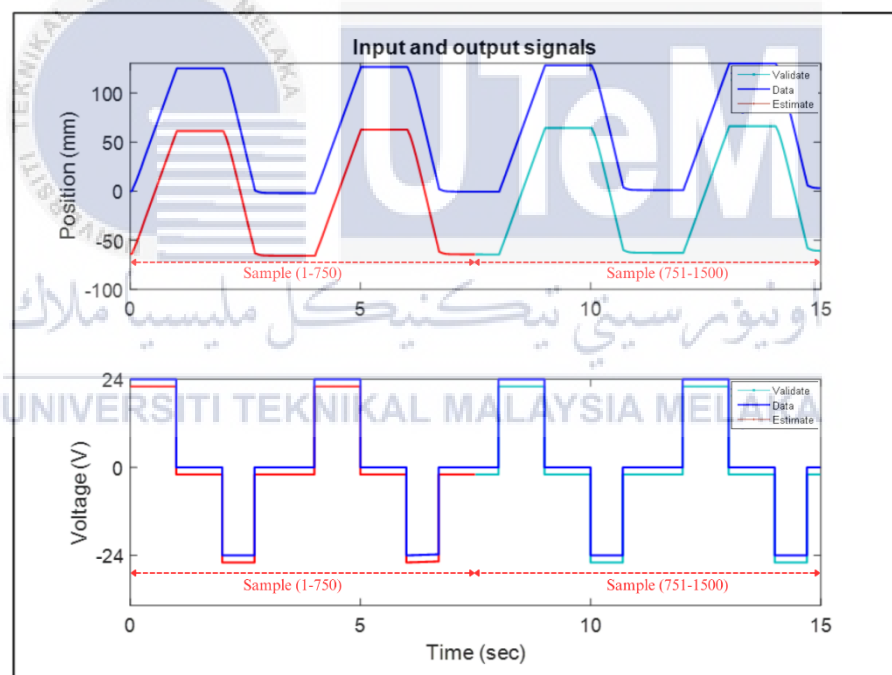


Figure 3.12 Estimation and validation process of measured data

The first 750 samples (marked as "Sample 1-750" in red) were used for model estimation, where the mathematical model representing the system's behavior was developed by analyzing the relationships between input signals (voltage) and output

responses (cylinder position). This step is crucial for constructing an accurate predictive model.

The remaining 750 samples (marked as "Sample 751-1500" in cyan) were used for model validation. This process involved comparing the model's predictions with the actual measured outputs to assess its accuracy and reliability. Validation ensures that the model performs well on new, unseen data, helping to identify and correct issues such as overfitting or underfitting.

The decision to use a 50/50 split for estimation and validation balances the need for sufficient data in both phases, minimizing bias and providing a solid statistical basis for performance evaluation. While 1500 data points are generally sufficient for many systems, the specific requirements of the system and the desired model accuracy influence this adequacy. More complex systems or higher accuracy needs may require additional data or advanced modeling techniques.

3.3.2 Model Structure Selection

In system identification, various parametric models can be used to represent a system, including Auto-Regressive with eXogenous input (ARX), Auto-Regressive Moving Average with eXogenous input (ARMAX), Output Error (OE), and Box-Jenkins (BJ) models. This study specifically focuses on ARX and ARMAX models to conduct the modeling of the IPA system, ultimately comparing them to determine the most suitable model. The choice to use ARX and ARMAX over BJ or OE models is based on several key factors.

Firstly, the ARX model is chosen for its simplicity and ease of implementation. The ARX model relies on past input and output data to predict future outputs, making

it straightforward to understand and apply. Its computational efficiency is also a significant advantage, allowing for rapid iterations and adjustments during the modeling process. Previous research has indicated that ARX models are particularly effective for systems that exhibit linear or near-linear behavior, which aligns with the initial assumptions about the IPA system.

However, recognizing that the IPA system might exhibit non-linearities and stochastic disturbances, the ARMAX model is also considered. The ARMAX model extends the ARX model by including a moving average component, which helps account for the aforementioned complexities. This additional feature allows the ARMAX model to provide a more accurate and robust representation of the system dynamics. The combination of ARX's simplicity and ARMAX's enhanced capability to handle non-linearities makes them a balanced choice for initial modeling efforts.

In contrast, the Box-Jenkins (BJ) and Output Error (OE) models, while powerful, are more complex and computationally intensive. The BJ model includes multiple parameters and structures to capture various system dynamics, which can be beneficial but also requires more data and computational resources. The OE model focuses on minimizing output error, which is useful for specific types of systems but might not provide the flexibility needed for the IPA system's expected non-linear behavior. Given the goals of the study and the available resources, ARX and ARMAX were deemed more suitable for effectively capturing the IPA system's dynamics while maintaining manageable complexity and computational demands.

The ARX model structure is a mathematical representation used in system identification to model the relationship between input and output data. The ARX

model is defined by two polynomials, $A(q)$ and $B(q)$. The following equation describes an ARX model.

$$A(q)y(n) = q^{-k}B(q)u(n) + e(n) = B(q)u(n - k) + e(n) \quad (3.1)$$

Figure 3.13 depicts the signal flow of an ARX model.

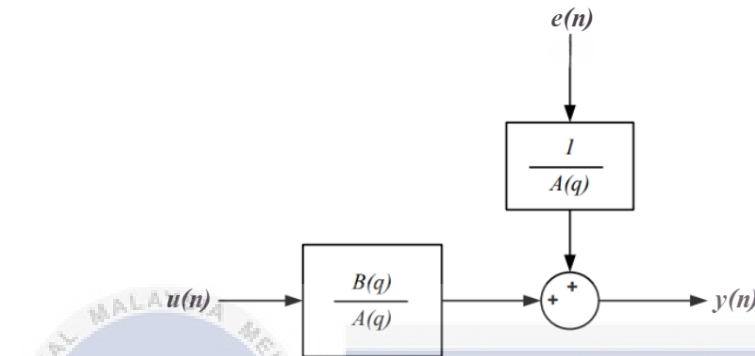


Figure 3.13 Block diagram of the ARX model structure

The ARMAX model is a type of linear dynamic system model that incorporates autoregressive (AR), moving average (MA), and exogenous (X) input components. It's particularly useful for modeling systems where past output values, past disturbances (or noise), and external input signals influence the current output. The general mathematical representation of an ARMAX model can be written as:

$$A(q)y(n) = q^{-k}B(q)u(n) + C(q)e(n) = B(q)u(n - k) + C(q)e(n) \quad (3.2)$$

The block diagram representation in Figure 3.14 helps visualize how these components interact.

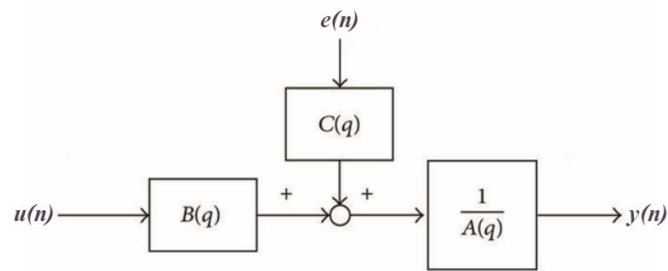


Figure 3.14 Block diagram of the ARMAX model structure

Define the orders of the polynomials. For ARX, specify $[na, nb, nk]$, where na is the order of the autoregressive part, nb is the order of the exogenous input part, and nk is the input delay. For ARMAX, include nc , the order of the moving average part, making it $[na, nb, nc, nk]$.



Figure 3.15 Orders of ARX model structure

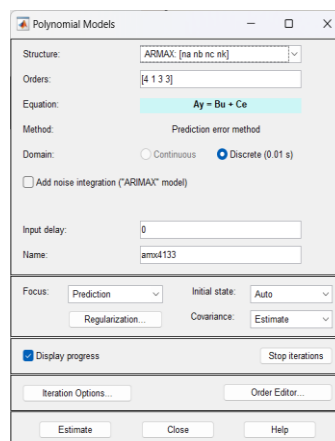


Figure 3.16 Orders of ARMAX model structure

3.3.3 Model Estimation

Model estimation involves determining the parameters of a mathematical model that best describes a system's behaviour based on observed data. The parameter estimation method involves determining the coefficients of these polynomials that best fit the observed data. For ARX models, the least squares method is typically used. This method minimizes the sum of the squared differences between the observed output and the predicted output, resulting in a set of linear equations that can be solved directly. For ARMAX models, the prediction error method is employed, which minimizes the prediction errors by considering both the system dynamics and the noise model. This involves more complex iterative optimization techniques to accurately estimate the parameters of the polynomials A, B and C.

Once the appropriate model structure and estimation method are selected, the estimation execution is carried out using tools System Identification Toolbox in MATLAB. In this process, the input-output data is loaded, the model orders are specified, and the estimation method is executed by clicking the 'Estimate' button. The toolbox computes the model parameters and fits the model to the observed data. Figure 3.17 showing the model info after the process of estimating. The result is a discrete-time transfer function of the IPA system, which describes the system's dynamics in the discrete domain. This transfer function is crucial for understanding how the system responds to different inputs and can be used for further analysis and control design. The transfer function is validated by comparing its output with actual system data, ensuring it accurately represents the IPA system.



Figure 3.17 The model info after the process of estimating

3.3.4 Model Validation

Model validation is a last crucial step in developing a mathematical model for an Intelligent Pneumatic Actuator (IPA) system using system identification techniques. The primary goal of this process is to ensure that the identified model accurately represents the real system. This is achieved by comparing the model's output with actual measured data, utilizing various validation criteria such as the percentage of best fit, mean square error (MSE), and final prediction error (FPE). Each of these metrics provides a different perspective on the model's performance, helping to verify its accuracy and reliability.

- Percentage of Best Fit:** This criterion measures how well the model output matches the actual data. It is expressed as a percentage, with higher percentages indicating a better fit. A model that closely follows the measured data points will have a higher percentage of best fit. It can be generally represented as in Equation 3.3.

$$Best\ Fit\ (\%) = \left(1 - \frac{|y - \hat{y}|}{|y - \bar{y}|}\right) \times 100 \quad (3.3)$$

y : Actual measured data.

\hat{y} : Predicted data from the model.

\bar{y} : Mean of the actual measured data.

- **Mean Square Error (MSE)**: MSE is a commonly used metric in model validation. It calculates the average of the squares of the errors, where the error is the difference between the actual and predicted values. Lower MSE values indicate a model that more accurately represents the system. It can be generally represented as in Equation 3.4.

$$MSE = \frac{1}{N} \sum_{i=1}^N (y_i - \hat{y}_i)^2 \quad (3.4)$$

N : Number of data points.

y_i : Actual measured data point at index i .

\hat{y}_i : Predicted data point at index i .

- **Final Prediction Error (FPE)**: FPE is another metric used to assess the model's accuracy. It considers the number of parameters in the model and provides an estimate of the prediction error. A lower FPE indicates a more reliable model.

$$FPE = \sigma^2 \left(\frac{N+d}{N-d}\right) \quad (3.5)$$

σ^2 : Variance of the residuals (errors).

N : Number of data points.

d : Number of parameters in the model.

In addition to these performance metrics, the stability of the discrete-time model is assessed through a Zero-Pole Plot. Stability is critical for ensuring the model's outputs remain bounded over time. For a discrete-time system to be stable, all poles of the identified model must lie within the unit circle in the complex plane, meaning their magnitudes must be less than one. If any pole is outside this circle, the system is deemed unstable. Therefore, by confirming that all poles are within the unit circle, the model's stability is assured, reinforcing its validity as a representation of the real IPA system.

3.4 Controller Design

In this study, a Proportional-Integral-Derivative (PID) controller was chosen to be used as it is an essential feedback control mechanism widely used in controlling the pneumatic positioning system. The PID controller continuously calculates the error value, which is the difference between a desired setpoint and a measured process variable. It then applies a correction based on proportional, integral, and derivative.

1. **Proportional (P) Component:** The proportional term produces an output value that is directly proportional to the current error value. It can be expressed as:

$$P = K_p \cdot e(t) \quad (3.6)$$

K_p : Proportional gain.

$e(t)$: Error at time t (difference between the desired setpoint and the actual value).

- 2. Integral (I) Component:** The integral term is concerned with the accumulation of past errors. If the error persists over time, the integral term accumulates this error and increases the controller output to eliminate the residual steady-state error. It is given by:

$$I = K_i \cdot \int_0^t e(\tau) d\tau \quad (3.7)$$

K_i : Integral gain.

$\int_0^t e(\tau) d\tau$: Integral of the error over time.

- 3. Derivative (D) Component:** The derivative term predicts the future trend of the error by considering its rate of change. It helps in damping the system response and reducing overshoot. It is formulated as:

$$D = K_d \cdot \frac{de(t)}{dt} \quad (3.8)$$

K_d : Derivative gain.

$\frac{de(t)}{dt}$: Rate of change of the error.

The overall PID control formula, which combines these three terms, is expressed in Equation 3.9. This formula combines the immediate error, the accumulated past errors, and the predicted future error to provide a comprehensive control output.

$$u(t) = K_p \cdot e(t) + K_i \cdot \int_0^t e(\tau) d\tau + K_d \cdot \frac{de(t)}{dt} \quad (3.9)$$

The block diagram of a PID controller typically includes a setpoint (desired value), an error calculation block, the PID controller block, the actuator/system, the process or plant, and a feedback loop as shown in Figure 3.18.

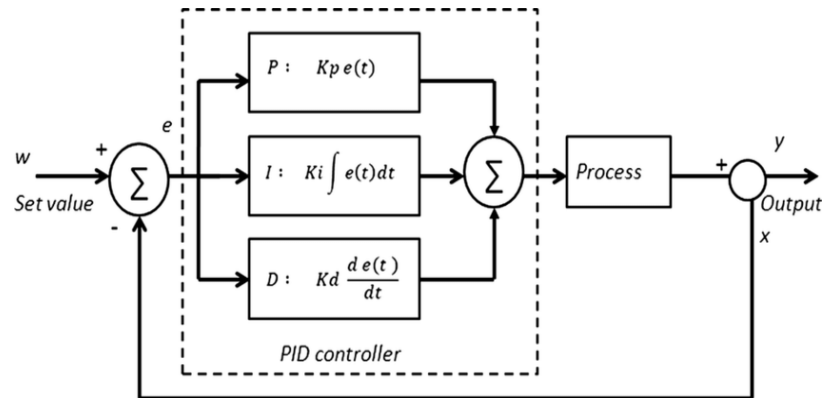


Figure 3.18

Block diagram of PID controller

The setpoint is compared to the process variable to calculate the error, which is then processed by the PID controller to produce the control output. This output is sent to the actuator, which adjusts the process variable. The process variable is then fed back into the system to continuously update the error calculation.

UNIVERSITI TEKNIKAL MALAYSIA MELAKA

PID controllers are favored for their robustness, versatility, and ease of implementation. They are effective and straightforward, making them suitable for a wide range of industrial applications. The combination of proportional, integral, and derivative actions ensures efficient and quick minimization of error, significantly improving system stability and dynamic performance when properly tuned. PID controllers are adaptable to various types of systems, both linear and non-linear, and their implementation is well-understood in both analog and digital forms. In IPA systems, PID controllers maintain precise control of the actuator's position or pressure by continuously adjusting control signals based on real-time feedback. This results in

high levels of accuracy and efficiency, essential for industrial automation and control applications where precision and reliability are critical.

3.5 Summary

This chapter thoroughly describes the processes and methods used in this study, focusing specifically on the modeling and control of the Intelligent Pneumatic Actuator (IPA) positioning system. The chapter starts with a detailed explanation of the procedures for modeling the IPA system using the system identification approach. Input and output data were collected through open-loop experimental tests on the IPA system. The study emphasized ARX and ARMAX models, comparing them to determine the best fit for the IPA system. The System Identification Tool in MATLAB was utilized to estimate the parameters of these models. After validating the identified model, it was used to develop a PID controller, which was the main controller for the IPA positioning system in this research. Suggestions for modifications to enhance the controller's performance are discussed in the subsequent chapter.

اوتنور سیتی بیکنیکل ملیسیا ملاک

UNIVERSITI TEKNIKAL MALAYSIA MELAKA

CHAPTER 4

RESULTS AND DISCUSSION



This chapter begins by presenting the results of system modeling. Transfer functions are formulated for ARX and ARMAX models with polynomial orders ranging up to the 5th order. For each derived transfer function, the percentage of best fit, mean square error (MSE), and final prediction error (FPE) are calculated. Additionally, Zero-Pole plots are created for each transfer function to assess stability. The results from the ARX and ARMAX models are then compared to determine which model order offers the best fit and stability. The most suitable transfer function is selected and implemented in SIMULINK for simulation experiments. The PID controller is then designed, and the simulation and actual experiments are carried out. The simulation results are compared with experimental data to evaluate how well the

transfer function represents the real system. Finally, the transient response is analyzed and discussed in this chapter.

4.1 System Modeling

4.1.1 Model Estimation

Table 4.1 shows the transfer functions for ARX and ARMAX models across different orders, ranging from the 1st to the 5th order.

Table 4.1 Transfer function of different orders ARX model

ARX model order	Transfer function
1 st order (ARX111)	$\frac{0.005829z^{-1}}{1 - 1.001z^{-1}}$
2 nd order (ARX212)	$\frac{0.001804z^{-2}}{1 - 1.702z^{-1} + 0.7021z^{-2}}$
3 rd order (ARX313)	$\frac{0.001381z^{-3}}{1 - 1.946z^{-1} + 1.128z^{-2} - 0.1813z^{-3}}$
4 th order (ARX413)	$\frac{0.001413z^{-3}}{1 - 1.991z^{-1} + 1.454z^{-2} - 0.6975z^{-3} + 0.2347z^{-4}}$
5 th order (ARX523)	$\frac{0.002496z^{-3} - 0.001391z^{-4}}{1 - 1.911z^{-1} + 1.212z^{-2} - 0.4495z^{-3} + 0.09224z^{-4} + 0.05635z^{-5}}$

For the ARX model in Table 4.1, each higher order introduces more complex polynomial coefficients, indicating increased accuracy and complexity in the model. For instance, the 1st order ARX model (ARX111) has a simple structure with a single

pole, whereas the 5th order ARX model (ARX523) incorporates five polynomial terms in the denominator and two in the numerator.

Table 4.2 Transfer function of different orders ARMAX model

ARMAX model order	Transfer function
1st order (AMX1111)	$\frac{0.005828z^{-1}}{1 - 1.001z^{-1}}$
2nd order (AMX2121)	$\frac{0.00133z^{-1}}{1 - 1.782z^{-1} + 0.7822z^{-2}}$
3rd order (AMX3121)	$\frac{0.001141z^{-1}}{1 - 2.011z^{-1} + 1.21 - 0.199z^{-3}}$
4th order (AMX4133)	$\frac{0.002164z^{-3}}{1 - 2.021z^{-1} + 1.965z^{-2} - 1.501z^{-3} + 0.5576z^{-4}}$
5th order (AMX5143)	$\frac{0.00185z^{-3}}{1 - 1.74z^{-1} + 0.973z^{-2} + 0.0271z^{-3} - 0.6969z^{-4} + 0.4369z^{-5}}$

Similarly, the ARMAX models show a progressive increase in complexity from the 1st to the 5th order in Table 4.2. The transfer functions of ARMAX models introduce additional parameters that account for moving average (MA) terms, which are not present in the ARX models. This inclusion makes ARMAX models potentially more accurate in capturing system behavior, especially in the presence of noise. The 5th order ARMAX model (AMX5143), for example, demonstrates a highly intricate structure with both the numerator and denominator featuring five terms, offering a refined fit at the cost of increased computational complexity.

4.1.2 Model Validation

Figure 4.1 shows the best fit results for ARX models with orders ranging from the 1st to the 5th, generated using the System Identification Tool in MATLAB. Each model's performance is evaluated by comparing the measured system output with the simulated model output. The best fit percentages are displayed alongside the graph, with the 4th order model (ARX413) achieving the highest fit at 91.79%, closely followed by the 5th order model (ARX523) at 91.71%. Interestingly, the 3rd order model (ARX313) also demonstrates a high fit at 91.65%, while the 2nd and 1st order models have lower fits at 91.48% and 90.12%, respectively.

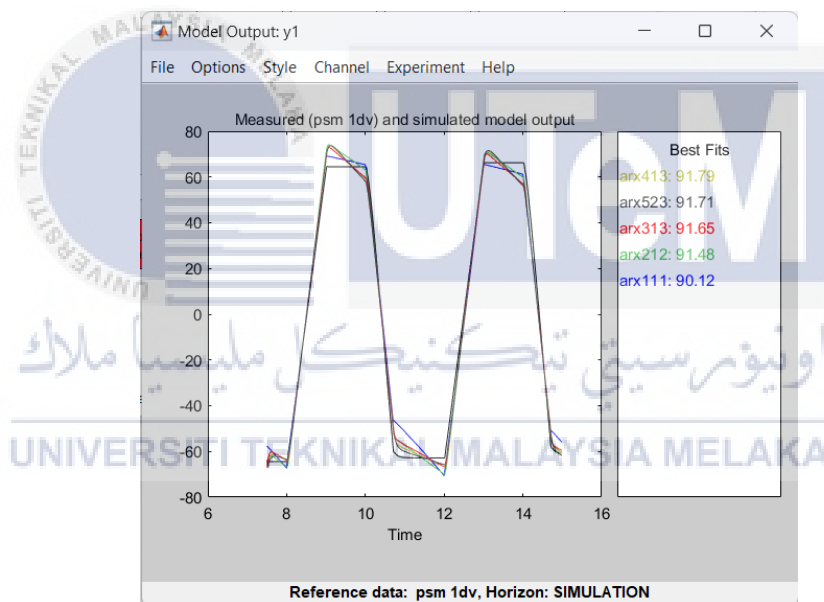


Figure 4.1 Plotting of best fit percentage for ARX model

This analysis shows that higher-order models do not always provide a significantly better fit compared to slightly lower-order models. For example, the 4th order model slightly outperforms the 5th order model, suggesting that adding more parameters does not always lead to substantial improvements in model accuracy. It also indicates a diminishing return in model performance with increasing complexity

beyond a certain point. Thus, while the 4th and 5th order models offer comparable accuracy, the 4th order model may be preferable due to its slightly better fit and potentially lower complexity, making it a more efficient choice for practical applications.

In Figure 4.2, the results reveal that the 4th order model (AMX4133) provides the highest fit percentage at 91.72%, suggesting it is the most accurate among the tested models. Following closely are 5th order model (AMX5143) and 3rd order model (AMX3121) with fits of 91.48% and 91.44%, respectively. Despite their slightly lower fit percentages, these models are also quite reliable. The 2nd order model (AMX2121) and 1st order model (AMX1111) with fits of 91.38% and 90.16%, respectively, show good performance but are less accurate compared to the top-performing models.

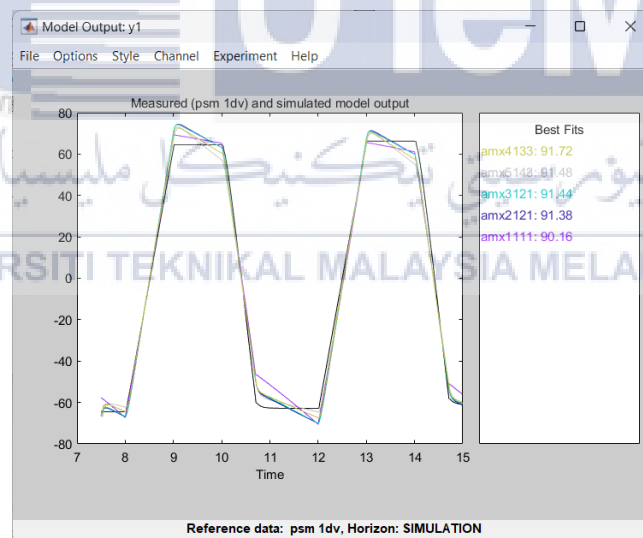


Figure 4.2 Plotting of best fit percentage for ARMAX model

Table 4.3 Summary of the best fit for ARX and ARMAX model

Order	ARX	ARMAX
1st Order	90.12%	90.16%
2nd Order	91.48%	91.38%
3rd Order	91.65%	91.44%
4th Order	91.79%	91.72%
5th Order	91.71%	91.48%

Table 4.3 summarizes the best fit percentages for ARX and ARMAX models of varying orders used in a system identification analysis. The ARX model of the 4th order exhibits the highest best fit at 91.79%, indicating that it most accurately replicates the measured data among the ARX models. Comparatively, the ARMAX models also show high accuracy, with the 4th order ARMAX model achieving a fit of 91.72%. This suggests that the ARX model, particularly the 4th order, offers a superior balance of complexity and accuracy for this specific system identification task. Thus, the 4th order ARX model is identified as the optimal model due to its highest fit percentage, making it the preferred choice for accurately modeling the system dynamics.

In analyzing the validation performance of ARX and ARMAX model structures, two key metrics were used: Final Prediction Error (FPE) and Mean Square Error (MSE). These metrics help in evaluating the accuracy and reliability of the models. The FPE is a criterion for model selection that estimates the expected

prediction error of the model when applied to a new data set. The MSE, on the other hand, measures the average squared difference between observed and predicted values, thus providing an indication of the model's accuracy.

The pole-zero plot is utilized to assess the stability of the models. The location of the poles in the plot indicates whether the system is stable or unstable. If all poles are within the unit circle, the system is stable. Conversely, poles outside the unit circle indicate instability.

Table 4.4 The validation performance of ARX model structure for five different model orders

Criteria	ARX model order				
	1 st order (ARX111)	2 nd order (ARX212)	3 rd order (ARX313)	4 th order (ARX413)	5 th order (ARX523)
Best fit	90.12%	91.48%	91.65%	91.79%	91.71%
Final Prediction Error (FPE)	0.0722	0.01285	0.016	0.01494	0.01427
Mean Square Error (MSE)	0.07163	0.01268	0.01571	0.01459	0.01382
Pole(s) location	1.0010	0.9997 0.7023	0.9970 0.6826 0.2664	0.9992 + 0.0000i 0.7836 + 0.0000i 0.1041 + 0.5375i 0.1041 - 0.5375i	0.9995 + 0.0000i 0.8536 + 0.0000i 0.1356 + 0.5395i 0.1356 - 0.5395i -0.2134 + 0.0000i
Stability	Unstable	Stable	Stable	Stable	Stable

Table 4.5 The validation performance of ARMAX model structure for five different model orders

Criteria	ARMAX model order				
	1 st order (AMX1111)	2 nd order (AMX2121)	3 rd order (AMX3121)	4 th order (AMX4133)	5 th order (AMX5143)
Best fit	90.16%	91.38%	91.44%	91.72%	91.48%
Final Prediction Error (FPE)	0.04371	0.01324	0.01296	0.01424	0.01375
Mean Square Error (MSE)	0.04325	0.01299	0.01265	0.01379	0.01321
Pole(s) location	1.0010	0.9991 0.7829	1.0000 0.7433 0.2677	0.1346 + 0.8504i 1.0000 0.1346 - 0.8504i 0.7535 + 0.0000i 0.9983 + 0.0000i	-0.7043 + 0.0000i 0.3039 + 0.8058i 0.3039 - 0.8058i 0.9997 + 0.0000i 0.8367 + 0.0000i
Stability	Unstable	Stable	Unstable	Stable	Stable

From Table 4.4 and 4.5, it is evident that the 4th order ARX model (ARX413) is chosen to represent the IPA system. This decision is based on its highest best-fit percentage (91.79%) and its stable nature, as confirmed by the pole locations (0.9992 + 0.0000i, 0.7836 + 0.0000i, 0.1041 + 0.5375i, 0.1041 - 0.5375i) all lying within the unit circle as shown in Figure 4.3. Additionally, the 4th order ARX model has low

FPE (0.01494) and MSE (0.01459), indicating a good balance between complexity and predictive accuracy. Therefore, considering the criteria of best fit, prediction accuracy, and stability, the 4th order ARX model is an optimal choice for representing the IPA system.

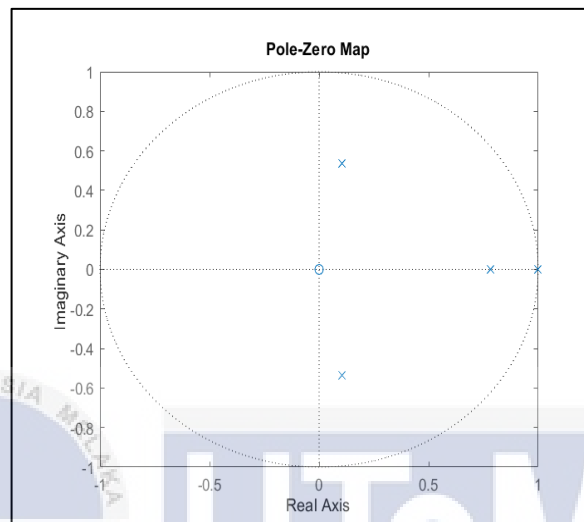


Figure 4.3 The pole-zero plot for 4th order of ARX model

4.2 Position Control of IPA system

4.2.1 Simulation Experiment of IPA system

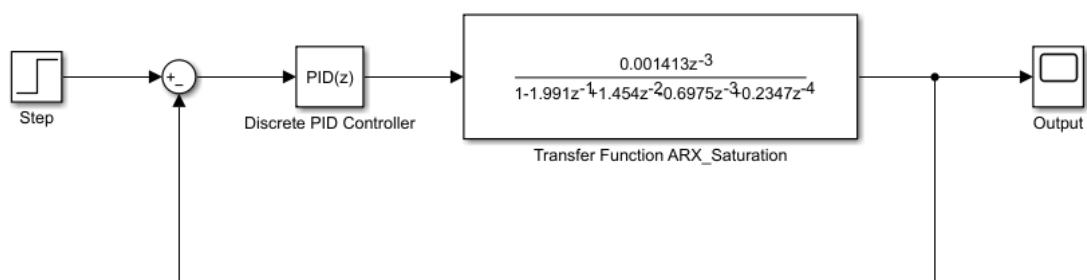


Figure 4.4 Control system of IPA system in simulation experiment

The Simulink diagram in Figure 4.4 illustrates a control system designed for an Intelligent Pneumatic Actuator (IPA) that manages the precise positioning of the actuator's cylinder stroke. The primary objective of this system is to achieve and

maintain specific stroke positions, responding to step inputs set at 50 mm, 100 mm, and 150 mm. This control is achieved through the implementation of a PID (Proportional-Integral-Derivative) controller, which plays a critical role in minimizing the error between the desired and actual positions. Here's a detailed breakdown of each component and its functionality within the system.

The step input block initiates the control process by providing a reference signal representing the desired stroke positions of 50 mm, 100 mm, and 150 mm. These step inputs simulate different target positions for the actuator's cylinder stroke, which the system must achieve. The use of step inputs is common in control systems as they allow for the evaluation of the system's transient and steady-state responses to sudden changes in the desired position.

Next, the summation block is where the error calculation occurs. This block receives the desired position from the step input and the actual position from the feedback loop. It computes the error by subtracting the actual position from the desired position. This error signal is fundamental to the control process, as it quantifies the deviation from the target position that the PID controller must correct. The continuous calculation of this error ensures that the system can dynamically respond to changes in the desired position or disturbances in the actual position.

The computed error signal is then sent to the PID controller, a crucial component of the control system. The PID controller operates in the discrete domain, indicated by the notation $PID(z)$. It uses proportional, integral, and derivative gains to process the error signal and generate an appropriate control signal. The combination of these three actions enables the PID controller to provide a robust control signal that minimizes the error effectively. Figure 4.5 shows the parameters of the PID controller.

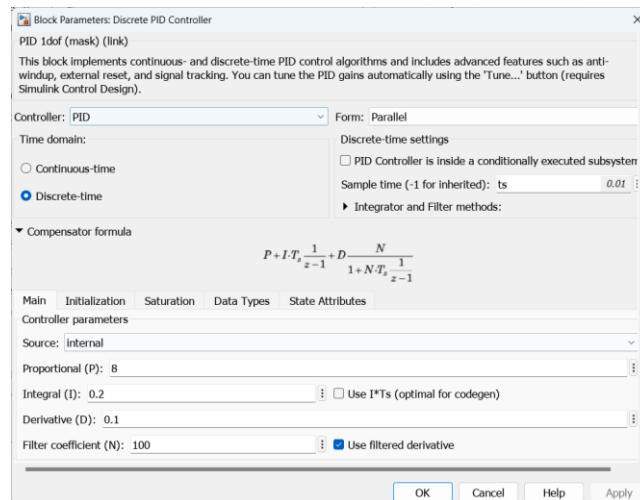


Figure 4.5 Controller parameters of the PID controller

The Controller Parameters section of the Discrete PID Controller block in Simulink specifies the internal gains and settings for the PID controller. The proportional gain (P) is set to 8, which determines the immediate response to the error signal. The integral gain (I) is 0.2, which accumulates the error over time to eliminate steady-state error. The derivative gain (D) is 0.1, which predicts future error based on its rate of change to improve stability and reduce overshoot.

Following the PID controller, the control signal is fed into the transfer function ARX_Saturation block, representing the dynamic model of the IPA system. The transfer function obtained from system modeling describes the relationship between the input control signal and the output stroke position. This ARX (Auto-Regressive with Exogenous Input) model encapsulates the system's dynamic behavior, capturing how the actuator responds over time. The term "Saturation" indicates that the actuator's output is limited, ensuring that it does not exceed certain predefined bounds, which is crucial for preventing damage and ensuring safe operation.

Finally, the feedback loop completes the closed-loop control system by feeding the actual stroke position back to the summation block. This continuous feedback allows the PID controller to adjust its control signal based on real-time measurements, ensuring that the actuator's position closely follows the desired position. The feedback loop is essential for maintaining system stability and achieving precise control. The output block displays the actual position of the cylinder stroke, providing a visual representation of the system's performance. By observing the output waveform, one can assess how effectively the PID controller maintains the desired stroke position, evaluates transient responses, and ensures minimal steady-state error.

4.2.1.1 Simulation Experiment Performances and Analysis

After running the simulation in Simulink, the output data for target positions of 50 mm, 100 mm, and 150 mm were exported to the MATLAB workspace for detailed analysis. This process involves capturing the system's response over time to each step input, allowing for a detailed examination of the transient performance metrics. In MATLAB, step response graphs were plotted for each target distance as shown in Figure 4.6, 4.7 and 4.8.

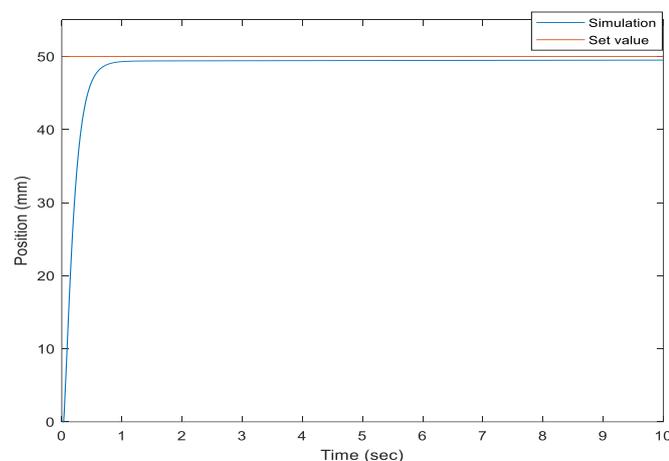


Figure 4.6 Step response at position distance of 50 mm

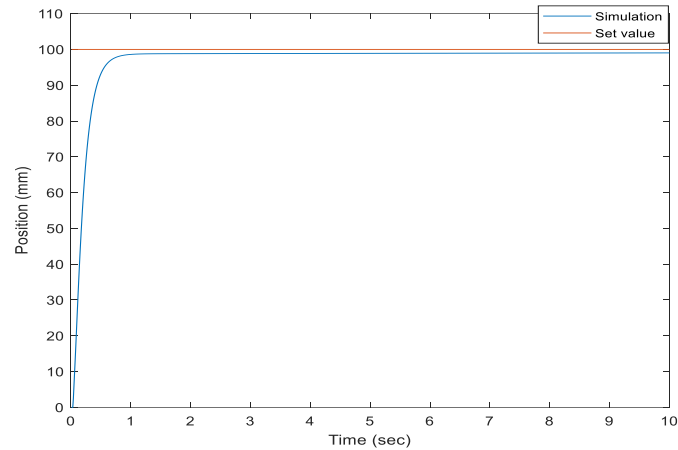


Figure 4.7 Step response at position distance of 100 mm

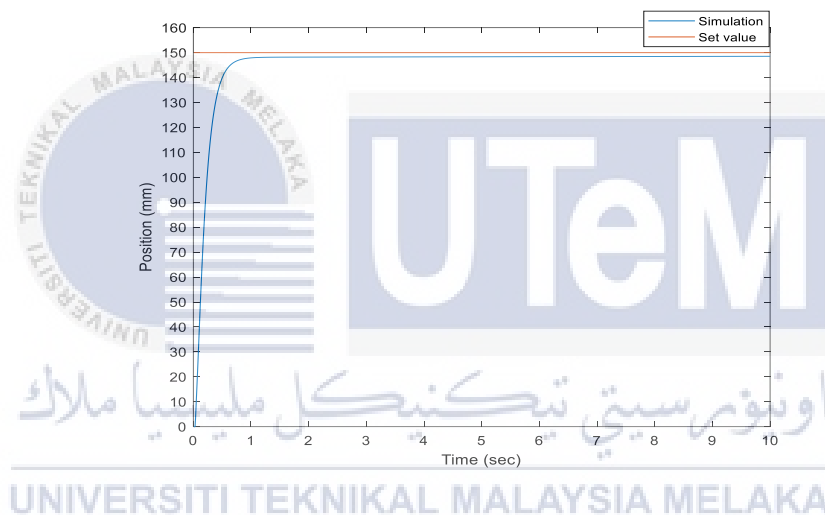


Figure 4.8 Step response at position distance of 150 mm

These graphs allow for a visual comparison of the system's performance against the desired targets. The set points, indicating the target positions of 50 mm, 100 mm, and 150 mm, are depicted in red on the graphs. The actual output from the simulation, which represents the real-time position of the actuator's stroke, is plotted in blue. By comparing the blue output lines to the red set points, one can assess the system's accuracy and responsiveness.

Table 4.6 Summary of the step response performances for position distance of 50 mm, 100 mm, and 150 mm in simulation experiment

Transient Performance	Distance (mm)		
	50	100	150
Rise Time, t_r (s)	0.3585	0.3585	0.3585
Settling Time, t_s (s)	0.6610	0.6610	0.6610
Overshoot, OS (%)	0	0	0
Steady-state error, e_{ss} (mm)	0.4855	0.971	1.4547

The table presents the transient performance metrics of the IPA system for three different target distances: 50 mm, 100 mm, and 150 mm. The key metrics assessed include rise time (t_r), settling time (t_s), overshoot (OS), and steady-state error (e_{ss}).

The rise time (t_r) is consistent across all target distances, recorded at 0.3585 seconds. This indicates that the time taken for the actuator to initially reach the target position is independent of the distance. A consistent rise time suggests that the system has a uniform initial response rate to changes in target position.

Similarly, the settling time (t_s) is uniform for all distances, measured at 0.6610 seconds. Settling time is the duration required for the system to remain within a certain error band around the target position after initial transients have decayed. The consistent settling time implies that the system's damping characteristics and response to disturbances are stable regardless of the stroke length.

The overshoot (OS) is zero for all distances, indicating that the system does not exceed the target position during its transient response. Zero overshoot is desirable in many control applications as it suggests a well-damped system with no risk of

exceeding the desired position, which could be critical for precision and safety in pneumatic actuators.

However, the steady-state error (e_{ss}) varies with the distance. At 50 mm, the steady-state error is 0.4855 mm, increasing to 0.971 mm at 100 mm, and further to 1.4547 mm at 150 mm. This indicates that as the target position increases, the system struggles more to reach the exact target, resulting in a higher final error. However, all steady-state errors fall within the $\pm 2\%$ acceptable range. This indicates that the control system maintains a satisfactory level of precision and accuracy across the different target positions.

4.2.2 Actual Experiment of IPA System

The actual experiment for position control of the IPA system was conducted to validate the simulation results. In the experimental setup as shown in Figure 4.9, the on-off control signal for the pneumatic valve is generated in Simulink and transmitted to the actual actuator system via a DAQ interface. This control signal modulates the valve, determining the airflow that drives the pneumatic cylinder to achieve the desired positions of 50 mm, 100 mm, and 150 mm.

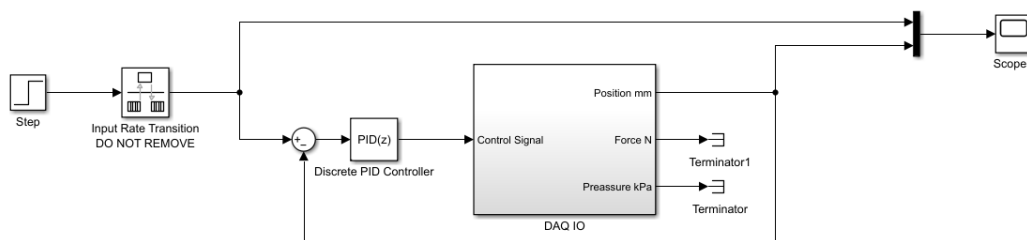


Figure 4.9 Control system of IPA system in actual experiment

The position of the pneumatic cylinder is continuously monitored using an optical encoder, which provides precise feedback on the current position of cylinder. The encoder's output, representing the actual position of the actuator, is then sent back to Simulink through the DAQ interface. This real-time feedback loop allows for continuous monitoring and adjustment of the control signal to ensure that the actuator follows the desired position trajectory accurately.

4.2.2.1 Actual Experiment Performances and Analysis

The step response for each target position was plotted as shown in Figure 4.10, 4.11 and 4.12 to compare the system's real-world performance against the expected outcomes from the simulation.

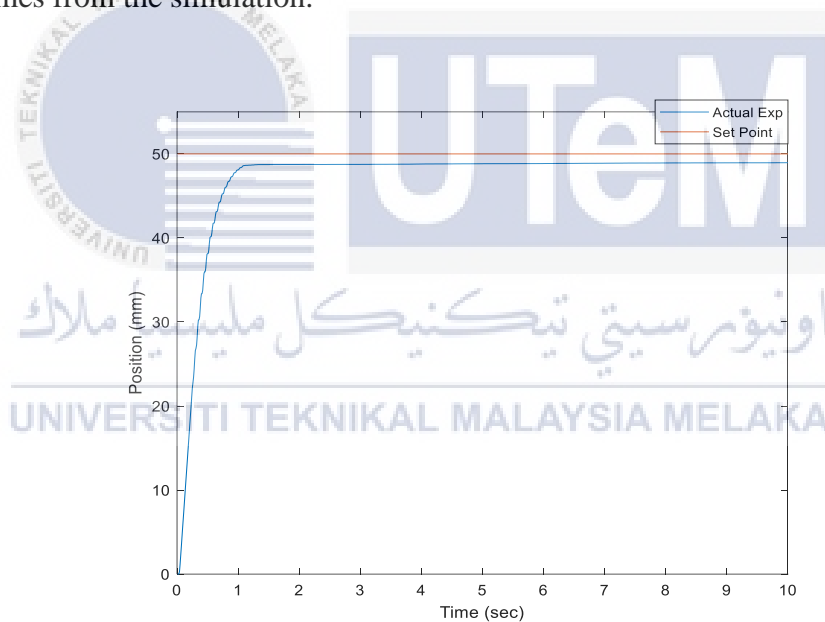


Figure 4.10 Step response at position distance of 50 mm

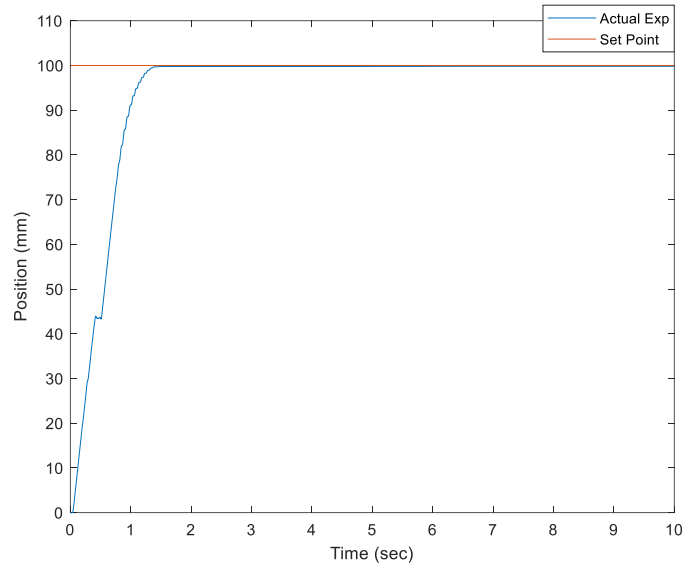


Figure 4.11 Step response at position distance of 100 mm

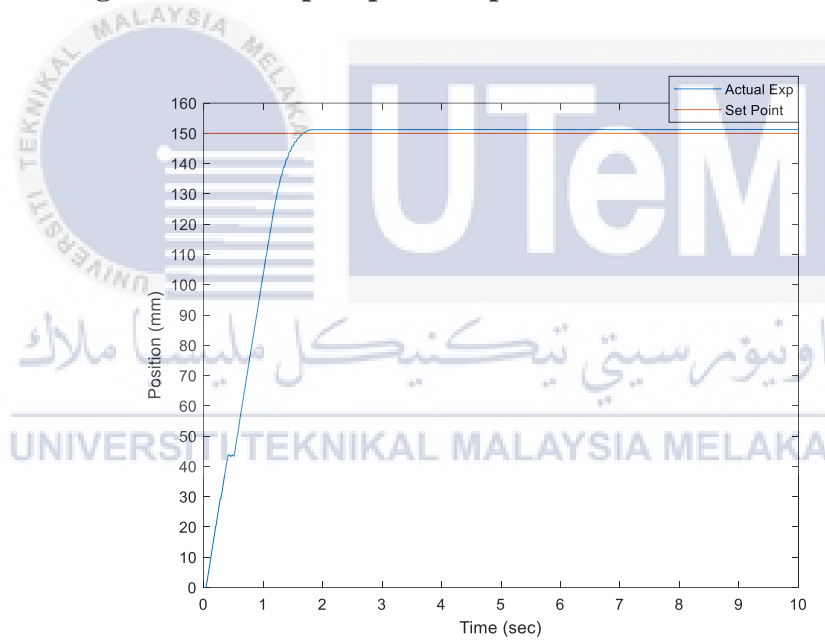


Figure 4.12 Step response at position distance of 150 mm

Table 4.7 Summary of the step response performances for position distance of 50 mm, 100 mm, and 150 mm in actual experiment

Transient Performance	Distance (mm)		
	50	100	150
Rise Time, t_r (s)	0.5971	0.8519	1.1511
Settling Time, t_s (s)	0.9630	1.2097	1.5672
Overshoot, OS (%)	0	0	0
Steady-state error, e_{ss} (mm)	0.9880	0.1860	1.2800

Table 4.7 presented an analysis of the step response performances for position control of a cylinder stroke at distances of 50 mm, 100 mm, and 150 mm using PID control. At a distance of 50 mm, the system exhibits the fastest rise time ($=0.5971$ s) and the quickest settling time ($=0.9630$ s). The overshoot is non-existent across all distances, which is indicative of the PID controller's effective tuning, preventing any oscillations or instability in the system. However, the steady-state error (e_{ss}) at 50 mm is relatively high (0.9880 mm), suggesting that while the system responds quickly, it does not reach the exact desired position as accurately at shorter distances.

As the position distance increases to 100 mm and 150 mm, the rise time and settling time both increase, with the rise time reaching 1.1511 seconds and the settling time extending to 1.5672 seconds at 150 mm. Despite the longer response times, the steady-state error varies, being the lowest at 100 mm (0.1860 mm) and highest at 150 mm (1.2800 mm). This variation indicates that the PID controller maintains better accuracy at intermediate distances, whereas the accuracy diminishes slightly at the

extremes. Overall, these results demonstrate the PID controller's capability to handle different stroke lengths effectively, though optimization might be needed to reduce steady-state errors, particularly at shorter and longer distances.

4.3 Position Control with Loading Effects

The experiment depicted in Figure 4.13 focuses on analysing the performance of a pneumatic lifting system under varying loading conditions. The pneumatic system's ability to precisely position loads of 1 kg, 3 kg, and 5 kg and a target position of 100 mm is assessed through real-time experiments, providing valuable insights into its transient response characteristics as shown in Figure 4.14, 4.15 and 4.16.



Figure 4.13 Pneumatic actuator with loads

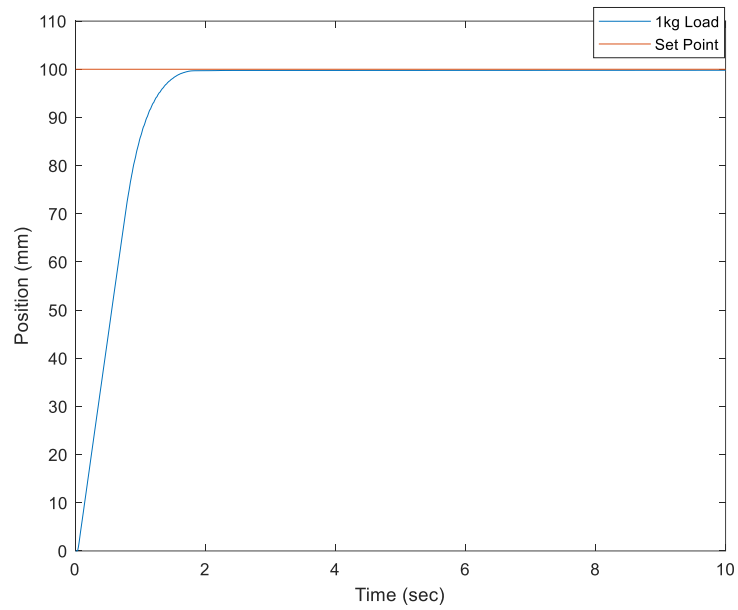


Figure 4.14 Step response with 1kg load

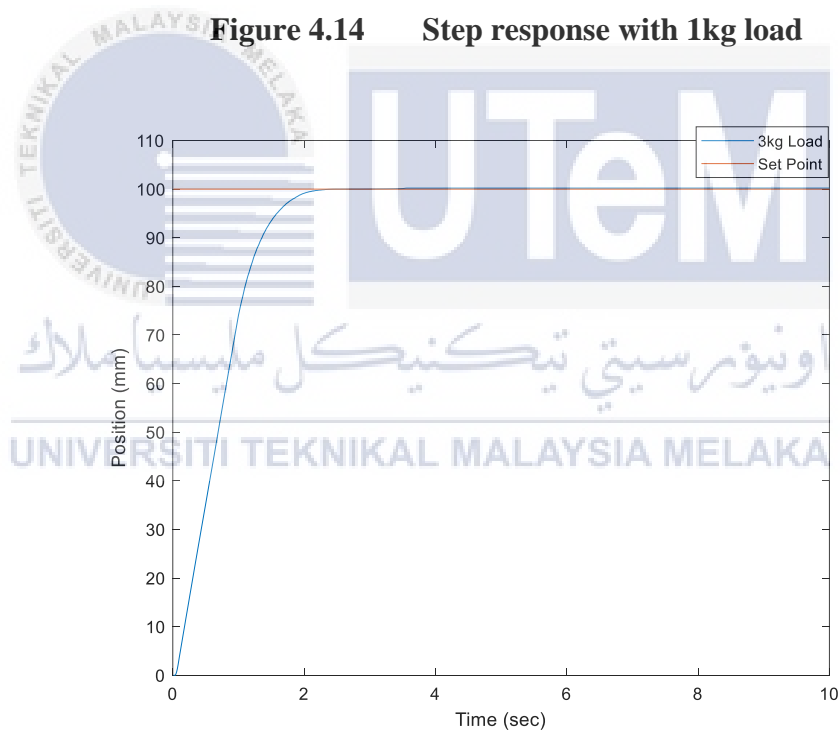


Figure 4.15 Step response with 3kg load

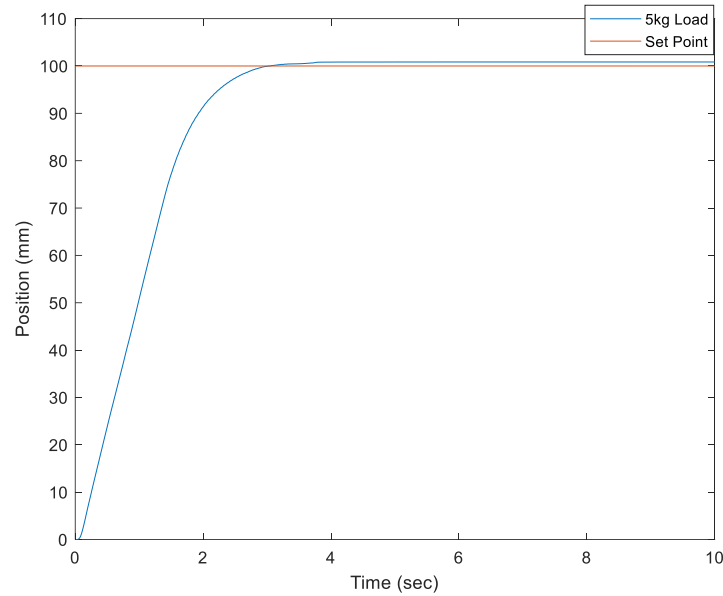


Figure 4.16 Step response with 5kg load

Table 4.8 Summary of the step response performances for position control with loading effects of 1kg, 3kg and 5kg

Transient Performance	Load (kg)		
	1	3	5
Rise Time, t_r (s)	0.9524	1.1847	1.7126
Settling Time, t_s (s)	1.4649	1.8517	2.7060
Overshoot, OS (%)	0	0	0
Steady-state error, e_{ss} (mm)	0.1520	0.2060	0.8520

The results summarized in Table 4.8 show that as the load increases, both the rise time (t_r) and settling time (t_s) of the system also increase. Specifically, the rise time increased from 0.9524 seconds for a 1 kg load to 1.7126 seconds for a 5 kg load. Similarly, the settling time rose from 1.4649 seconds to 2.7060 seconds over the same

range. This trend indicates that the system requires more time to reach and stabilize at the desired position as the load becomes heavier. Despite this increase in response time, the system maintains zero overshoot (**OS**), demonstrating effective control over the positioning without exceeding the target position.

The steady-state error (e_{ss}) also exhibits an increasing trend with heavier loads, from 0.1520 mm for a 1 kg load to 0.8520 mm for a 5 kg load. While the system shows a higher steady-state error with increasing load, it remains within acceptable limits, highlighting the pneumatic system's capability to maintain precision under varying payloads. These results suggest that while the system's response time and steady-state error are affected by load variations, it can still achieve accurate positioning without overshoot, demonstrating robust performance in handling different loads. Future improvements could focus on optimizing the control strategy to further reduce the rise and settling times and minimize steady-state error for heavier loads.

4.4 Environment and Sustainability

The development of a Proportional-Integral-Derivative (PID) controller for a pneumatic lifting system showcases a comprehensive approach to evaluating and enhancing sustainability impacts in industrial contexts. The project's focus on precise control addresses complex and infrequently encountered issues such as the non-linear behaviour of pneumatic systems, which often lead to energy inefficiencies and safety risks. By employing advanced system identification techniques and a robust PID control strategy, the project minimizes energy wastage and reduces the environmental footprint associated with the frequent maintenance and replacement of pneumatic components. This not only conserves resources but also extends the operational lifespan of equipment, promoting sustainable industrial practices.

Moreover, the enhanced precision and consistency of the pneumatic lifting system significantly improve workplace safety, addressing societal concerns related to occupational health. By reducing the potential for accidents and equipment failures, the project contributes to a safer working environment, aligning with the goal of protecting human health and well-being. The adaptive nature of the control strategy ensures that the system can handle variations in load and operating conditions, demonstrating resilience and reliability in diverse industrial settings.



CHAPTER 5

CONCLUSION AND FUTURE WORKS



5.1 Conclusion

In conclusion, the project successfully developed a robust mathematical model of a pneumatic lifting system using a 4th order ARX model through System Identification, demonstrating high predictive accuracy and stability. The PID controller designed and implemented in MATLAB/Simulink achieved precise control, providing fast response times without overshoot for position distances of 50 mm, 100 mm, and 150 mm. The system maintained steady-state accuracy despite load variations from 1 kg to 5 kg, with consistent zero overshoot and acceptable steady-state errors, validating the effectiveness of the PID-based control strategy. These results highlight the potential for PID controllers to ensure reliable and precise pneumatic positioning in diverse industrial applications, with future work focusing on further optimization and advanced PID techniques for enhanced performance.

5.2 Future Works

5.2.1 Nonlinear Modeling

Although the current project focused on linear model structures such as ARX and ARMAX, real-world pneumatic systems often exhibit nonlinear behaviors, including air compressibility, friction effects, and valve dead-zone. Future work could involve developing nonlinear models using advanced techniques like NARX (Nonlinear ARX) or machine learning methods. These nonlinear models would provide a more accurate representation of the pneumatic system dynamics, capturing the complexities and inherent nonlinearities of the physical processes. By considering these nonlinearities, the control strategies can be significantly improved, leading to better performance and reliability in various operating conditions.

5.2.2 Advanced PID Control Techniques

Future research should explore advanced PID control techniques to enhance the system's adaptability and precision. Adaptive PID control can be implemented for real-time parameter adjustment, allowing the system to maintain optimal performance despite changes in load or external disturbances. Fuzzy logic-based PID controllers can be employed to handle nonlinearities, providing smoother and more effective control by dynamically adjusting PID parameters based on a set of fuzzy rules. Additionally, neural network PID tuning can offer enhanced adaptability by learning and adjusting to the system's behavior over time, further improving control accuracy and response.

REFERENCES

- [1] “What exactly is lifting equipment and what tasks can it handle?”
https://hovmand.com/en_gb/insights/blog/insights/blog/what-exactly-is-lifting-equipment-and-what-tasks-can-it-handle (accessed May. 10, 2024).
- [2] “Official Website Department of Occupational Safety and Health - Lifting Works.” <https://www.dosh.gov.my/index.php/construction-safety-v/lifting-works> (accessed May. 16, 2024).
- [3] M. Papoutsidakis, A. Srivastava, and S. Chowdhary, “Displacement Sensors for Linear Electrical, Hydraulic and Pneumatic Actuators,” *Proc. - 2019 Amity Int. Conf. Artif. Intell. AICAI 2019*, pp. 269–273, 2019, doi: 10.1109/AICAI.2019.8701227.
- [4] V. Boyko and J. Weber, “Energy Efficiency of Pneumatic Actuating Systems with Pressure-Based Air Supply Cut-Off,” *Actuators*, vol. 13, no. 1, Jan. 2024, doi: 10.3390/act13010044.
- [5] M. S. Xavier *et al.*, “Soft Pneumatic Actuators: A Review of Design, Fabrication, Modeling, Sensing, Control and Applications,” *IEEE Access*, vol.

- 10, pp. 59442–59485, 2022, doi: 10.1109/ACCESS.2022.3179589.
- [6] J. Pustavrh, M. Hočevar, P. Podržaj, A. Trajkovski, and F. Majdič, “Comparison of hydraulic, pneumatic and electric linear actuation systems,” *Sci. Rep.*, vol. 13, no. 1, pp. 1–13, 2023, doi: 10.1038/s41598-023-47602-x.
- [7] D. Yamaguchi, T. Hanaki, Y. Ishino, M. Hara, M. Takasaki, and T. Mizuno, “Concept and prototype of soft actuator for liquid nitrogen temperature environments,” *J. Robot. Mechatronics*, vol. 32, no. 5, pp. 1019–1026, 2020, doi: 10.20965/jrm.2020.p1019.
- [8] B. Rouzbeh, G. M. Bone, G. Ashby, and E. Li, “Design, Implementation and Control of an Improved Hybrid Pneumatic-Electric Actuator for Robot Arms,” *IEEE Access*, vol. 7, pp. 14699–14713, 2019, doi: 10.1109/ACCESS.2019.2891532.
- [9] R. Abela, P. Refalo, M. Borg, and E. Francalanza, “Pneumatic Control for Sustainable Compressed Air Systems: Multi-criteria Optimisation for Energy Efficient Production,” *Procedia CIRP*, vol. 122, pp. 247–252, 2024, doi: 10.1016/j.procir.2024.01.035.
- [10] V. Boyko, S. Hülsmann, and J. Weber, “Comparative Analysis of Actuator Dimensioning Methods in Pneumatics,” *Proc. ASME/BATH 2021 Symp. Fluid Power Motion Control.*, Oct. 2021, doi: 10.1115/FPMC2021-68674.
- [11] Z. Liu, X. Yin, K. Peng, X. Wang, and Q. Chen, “Soft pneumatic actuators adapted in multiple environments: A novel fuzzy cascade strategy for the dynamics control with hysteresis compensation,” *Mechatronics*, vol. 84, p.

102797, Jun. 2022, doi: 10.1016/J.MECHATRONICS.2022.102797.

- [12] K. Osman, A. A. M. Faudzi, M. F. Rahmat, C. C. Kai, and K. Suzumori, "Design and development of Ankle-Foot Rehabilitation Exerciser (AFRE) system using pneumatic actuator," *J. Telecommun. Electron. Comput. Eng.*, vol. 10, no. 2–8, pp. 137–143, 2018.
- [13] M. N. Muftah, A. A. M. Faudzi, S. Sahlan, and S. Mohamaddan, "Intelligent Position Control for Intelligent Pneumatic Actuator with Ball-Beam (IPABB) System," *Appl. Sci.*, vol. 12, no. 21, 2022, doi: 10.3390/app122111089.
- [14] K. Osman, A. N. Ahmad Sukri, S. F. Sulaiman, A. R. Azira, and M. F. Faujan, "Predictive controller with Kalman filter for Intelligence Pneumatic Actuator (IPA)," *J. Adv. Manuf. Technol.*, vol. 13, no. Special Issue 2, pp. 1–10, 2019.
- [15] S. F. Sulaiman, M. F. Rahmat, A. A. M. Faudzi, and K. Osman, "A new technique to reduce overshoot in pneumatic positioning system," *Telkonnika (Telecommunication Comput. Electron. Control.)*, vol. 17, no. 5, pp. 2607–2616, 2019, doi: 10.12928/TELKOMNIKA.v17i5.12807.
- [16] F. H. Khong *et al.*, "Linear ARX modelling of pneumatic actuator system," *Sens. Instrum. Syst.*, no. UTHM, pp. 125–143, 2022.
- [17] M. N. Muftah, W. L. Xuan, and A. 'Athif M. Faudzi, "ARX, ARMAX, Box-Jenkins, Output-Error, and Hammerstein Models for Modeling Intelligent Pneumatic Actuator (IPA) System," *J. Integr. Adv. Eng.*, vol. 1, no. 2, pp. 81–88, 2021, doi: 10.51662/jiae.v1i2.18.
- [18] M. Awad, S. Rabbo, and M. El-Arabi, "Identification and analysis of Servo-

- Pneumatic System using mixed reality environment.,” *J. Int. Soc. Sci. Eng.*, vol. 0, no. 0, pp. 0–0, 2021, doi: 10.21608/jisse.2021.95202.1042.
- [19] M. Etewa, G. Elnashar, A. Kamel, and H. Hendy, “Design And Implementation of Embedded Servo Control System for a high maneuvering Ariel Vehicle,” *J. Eng. Sci. Mil. Technol.*, vol. 0, no. 0, pp. 0–0, 2022, doi: 10.21608/ejmtc.2022.166266.1238.
- [20] L. Kotkas, N. Zhurkin, A. Donskoy, and A. Zharkovskij, “Design and Mathematical Modeling of a Pneumatic Artificial Muscle-Actuated System for Industrial Manipulators,” *Machines*, vol. 10, no. 10, 2022, doi: 10.3390/machines10100885.
- [21] A. Mandali and L. Dong, “Modeling and Cascade Control of a Pneumatic Positioning System,” *J. Dyn. Syst. Meas. Control. Trans. ASME*, vol. 144, no. 6, 2022, doi: 10.1115/1.4053966.
- [22] H. Qi, G. M. Bone, and Y. Zhang, “Position control of pneumatic actuators using three-mode discrete-valued model predictive control,” *Actuators*, vol. 8, no. 3, 2019, doi: 10.3390/ACT8030056.
- [23] M. Youssry, W. Elmayyah, and M. Mabrouk, “Position control of a pneumatic cylinder actuator using modified PWM algorithm,” *J. Eng. Sci. Mil. Technol.*, vol. 4, no. 1, pp. 121–126, 2020, doi: 10.21608/ejmtc.2020.31861.1145.
- [24] M. I. P. Azahar, A. Irawan, R. M. Taufika, and M. H. Suid, “Position Control of Pneumatic Actuator Using Cascade Fuzzy Self-adaptive PID,” *Lect. Notes Electr. Eng.*, vol. 632, pp. 3–14, 2020, doi: 10.1007/978-981-15-2317-5_1.

- [25] Y. Elsayed, M. Hammam, G. Mousa, and A. A. Morgan, "Simulation Study and Experimental Position Control of Pneumatic Cylinder Using Sliding Mode Control with on/off Control Valves," *Port-Said Eng. Res. J.*, vol. 0, no. 0, pp. 0–0, 2020, doi: 10.21608/pserj.2020.22883.1030.
- [26] W. Essmat Abdul-Lateef, N. A. Glebov, N. Hamed Farhood, A. H. Khdir, and D. H. Shaker, "Modelling and Controlling of position for electro-pneumatic system using Pulse-Width-Modulation (PWM) techniques and Fuzzy Logic controller," *IOP Conf. Ser. Mater. Sci. Eng.*, vol. 765, no. 1, 2020, doi: 10.1088/1757-899X/765/1/012020.
- [27] K. N. Kamaludin, L. Abdullah, S. N. S. Salim, Z. Jamaludin, and M. N. Maslan, "Improvement of a Proportional-Integral (PI) Controller for a Servo Pneumatic Actuator by Adapting Zero-Compensator Placement Method," *2021 IEEE 12th Control Syst. Grad. Res. Colloquium, ICSGRC 2021 - Proc.*, no. April 2022, pp. 222–226, 2021, doi: 10.1109/ICSGRC53186.2021.9515278.
- [28] S. F. Sulaiman, M. F. Rahmat, A. A. Faudzi, K. Osman, and N. H. Sunar, "Enhancement in pneumatic positioning system using nonlinear gain constrained model predictive controller: Experimental validation," *Indones. J. Electr. Eng. Comput. Sci.*, vol. 23, no. 3, pp. 1385–1397, 2021, doi: 10.11591/ijeecs.v23.i3.pp1385-1397.
- [29] M. N. Muftah, A. Athif, M. Faudzi, S. Sahlan, and M. Shouran, "Modeling and Fuzzy FOPID Controller Tuned by PSO for Pneumatic Positioning System," pp. 1–19, 2022.
- [30] M. Zhu, Z. Xu, Z. Zang, and X. Dong, "Design of FOPID Controller for

Pneumatic Control Valve Based on Improved BBO Algorithm,” *Sensors*, vol. 22, no. 17, 2022, doi: 10.3390/s22176706.

- [31] M. N. Muftah, A. A. M. Faudzi, S. Sahlan, and S. Mohamaddan, “Fuzzy Fractional Order PID Tuned via PSO for a Pneumatic Actuator with Ball Beam (PABB) System,” *Fractal Fract.*, vol. 7, no. 6, pp. 1–31, 2023, doi: 10.3390/fractalfract7060416.



APPENDICES

Appendix A NI SCB-68A PINOUT



ANALOG	ANALOG/ DIGITAL	DIGITAL	DIGITAL				
68	AI 0 (AI 0+)	59	AI GND	51	P0.5	1	PFI 14 / P2.6
34	AI 8 (AI 0-)	25	AI 6 (AI 6+)	17	P0.1	35	D GND
67	AI GND	58	AI 14 (AI 6-)	50	D GND	2	PFI 12 / P2.4
33	AI 1 (AI 1+)	24	AI GND	16	P0.6	36	D GND
66	AI 9 (AI 1-)	57	AI 7 (AI 7+)	49	P0.2	3	PFI 9 / P2.1
32	AI GND	23	AI 15 (AI 7-)	15	D GND	37	PFI 8 / P2.0
65	AI 2 (AI 2+)	56	AI GND	48	P0.7	4	D GND
31	AI 10 (AI 2-)	22	AO 0	14	+5V	38	PFI 7 / P1.7
64	AI GND	55	AO GND	47	P0.3	5	PFI 6 / P1.6
30	AI 3 (AI 3+)	21	AO 1	13	D GND	39	PFI 15 / P2.7
63	AI 11 (AI 3-)	54	AO GND	46	PFI 11 / P2.3	6	PFI 5 / P1.5
29	AI GND	20	APFI 0	12	D GND	40	PFI 13 / P2.5
62	AI SENSE	53	D GND	45	PFI 10 / P2.2	7	D GND
28	AI 4 (AI 4+)	19	P0.4	11	PFI 0 / P1.0	41	PFI 4 / P1.4
61	AI 12 (AI 4-)	52	P0.0	44	D GND	8	+5V
27	AI GND	18	D GND	10	PFI 1 / P1.1	42	PFI 3 / P1.3
60	AI 5 (AI 5+)					9	D GND
26	AI 13 (AI 5-)					43	PFI 2 / P1.2

SCB-68A Quick Reference Label

NI 6251/6255/6259/6281/6289 (M Series) Devices
 NI 635x/636x/6375/6376/6378 (X Series) Devices
 CONNECTOR 0 (AI 0-15)

